AD_____

CONTRACT NUMBER DAMD17-96-C-6082

TITLE: Virus-Targeted Therapeutic for Breast Cancer

PRINCIPAL INVESTIGATOR: Douglas V. Faller, Ph.D.

CONTRACTING ORGANIZATION: Boston University School of Medicine
Boston, Massachusetts 02118

REPORT DATE: August 1999

TYPE OF REPORT: Final

PREPARED FOR: Commander
U.S. Army Medical Research and Materiel Command
Fort Detrick, Frederick, Maryland 21702-5012

REPORT DOCUMENTATION PAGE

Form Approved
OMB No. 0704-0188

1. AGENCY USE ONLY *(Leave blank)*	2. REPORT DATE	3. REPORT TYPE AND DATES COVERED
	August 1999	Final (15 Jul 96 - 14 Jul 99)

4. TITLE AND SUBTITLE
Virus-Targeted Therapeutic for Breast Cancer

5. FUNDING NUMBERS
DAMD17-96-C-6082

6. AUTHOR(S)
Douglas V. Faller, Ph.D.

7. PERFORMING ORGANIZATION NAME(S) AND ADDRESS(ES)
Boston University School of Medicine
Boston, Massachusetts 02118

E*Mail: dfaller@bu.edu

8. PERFORMING ORGANIZATION REPORT NUMBER

9. SPONSORING/MONITORING AGENCY NAME(S) AND ADDRESS(ES)
Commander
U.S. Army Medical Research and Materiel Command
Fort Detrick, Frederick, Maryland 21702-5012

10. SPONSORING/MONITORING AGENCY REPORT NUMBER

11. SUPPLEMENTARY NOTES

12a. DISTRIBUTION / AVAILABILITY STATEMENT
Approved for public release; distribution unlimited

12b. DISTRIBUTION CODE

13. ABSTRACT *(Maximum 200*

We have developed small molecules to alter the transcriptional response of viral genes for the treatment of human breast cancer. We have previously successfully used these compounds as therapeutic agents for gene regulation in humans. The transcriptional activity of certain viral genes, including the Epstein-Barr virus (EBV) Thymidine Kinase (TK) gene, is enhanced by these drugs. This work has led to the development of a virus-directed strategy for treating lymphoid malignancies associated with EBV. Exposure to Arginine Butyrate induces the latent TK gene in EBV-infected cells, resulting in susceptibility to ganciclovir. The presence of the Epstein-Barr virus in breast carcinomas of varying histology is strikingly high, raising the possibility of a therapeutic strategy for EBV(+) breast cancers. Our approach initially involves investigation of EBV sequences in breast cancer cell lines and specimens, determination of whether treatment with Arginine Butyrate will induce the viral thymidine kinase gene, and determination *in vitro* of whether the induction of the TK gene and gene product makes the breast cancer cells now susceptible to ganciclovir. We have initiated a clinical trial of an EBV-based strategy for treating cancers, including breast cancer, and shown safety and efficacy in early studies.

14. SUBJECT TERMS	15. NUMBER OF PAGES
Breast Cancer	80
	16. PRICE CODE

17. SECURITY CLASSIFICATION OF REPORT	18. SECURITY CLASSIFICATION OF THIS PAGE	19. SECURITY CLASSIFICATION OF ABSTRACT	20. LIMITATION OF ABSTRACT
Unclassified	Unclassified	Unclassified	Unlimited

FOREWORD

Opinions, interpretations, conclusions and recommendations are those of the author and are not necessarily endorsed by the U.S. Army.

____ Where copyrighted material is quoted, permission has been obtained to use such material.

____ Where material from documents designated for limited distribution is quoted, permission has been obtained to use the material.

____ Citations of commercial organizations and trade names in this report do not constitute an official Department of Army endorsement or approval of the products or services of these organizations.

____ In conducting research using animals, the investigator(s) adhered to the "Guide for the Care and Use of Laboratory Animals," prepared by the Committee on Care and use of Laboratory Animals of the Institute of Laboratory Resources, national Research Council (NIH Publication No. 86-23, Revised 1985).

DF ✓ For the protection of human subjects, the investigator(s) adhered to policies of applicable Federal Law 45 CFR 46.

DF ____ In conducting research utilizing recombinant DNA technology, the investigator(s) adhered to current guidelines promulgated by the National Institutes of Health.

DF ____ In the conduct of research utilizing recombinant DNA, the investigator(s) adhered to the NIH Guidelines for Research Involving Recombinant DNA Molecules.

____ In the conduct of research involving hazardous organisms, the investigator(s) adhered to the CDC-NIH Guide for Biosafety in Microbiological and Biomedical Laboratories.

T Dwight Tan 9/8/99

PI - Signature Date

Table of Contents

Progress Report

Douglas V. Faller, Ph.D., M.D.

Virus-Targeted Therapeutic for Breast Cancer

5. Introduction

We have previously developed families of small molecules (butyrate-related compounds) to alter the transcriptional response of cellular genes, and this proposal utilizes this same strategy for induction of viral genes for the treatment of virally-associated human breast cancer. The transcriptional activity of certain viral genes, including the Epstein-Barr viral (EBV) *Thymidine Kinase* (*TK*) gene, is enhanced by these butyrates. This work has led to the development of a virus-directed strategy for treating lymphoid malignancies associated with EBV, including Hodgkin's disease, Burkitt's lymphoma, certain non-Hodgkin's lymphomas, and B cell lymphoproliferative disorders. The Epstein-Barr virus, which is associated with these disorders is not normally susceptible to the nucleoside anti-viral agents, like ganciclovir (GCV), which require an active viral Thymidine Kinase for its activity. Exposure to Arginine Butyrate, however, induces the latent Thymidine Kinase gene in Epstein-Barr virus-infected cells, resulting in susceptibility to GCV. We have proposed and successfully carried out (under FDA approval) the treatment of these lymphoid malignancies associated with the Epstein-Barr virus in pilot clinical trials. We are also approved by the FDA to treat any EBV(+) solid tumor.

Epithelial cells, as well as B cells, are susceptible to Epstein-Barr virus infection. Epstein-Barr virus can be found in a wide distribution of lymphoepithelioma-like carcinomas, including the malignant cells of breast cancer. The presence of the Epstein-Barr virus in breast carcinomas of varying histology is strikingly high. EBV is present in 60 % of breast cancers in some studies, and more recently was shown to be present in 51% of invasive carcinomas (I Magrath, K Bhatia. Breast cancer: a new Epstein-Barr virus-associated disease? Journal of the National Cancer Institute, 1999, 91:1349-1350. M Bonnet, JM Guinebretiere, E Kremmer, V Grunewald, E Benhamou, G Contesso, I Joab. Detection of Epstein-Barr virus in invasive breast cancers. Journal of the National Cancer Institute, 1999, 91:1376-1381). It is most prevalent in medullary carcinomas and is also quite frequent in the (more prevalent) invasive ductal cancers (of 48 invasive ductal carcinomas, 19 were EBV(+)). In addition to EBV genomic DNA detected by PCR, latent membrane viral protein was detected by immunohistology in the epithelial breast tumor cells (but not in surrounding lymphoid cells). No EBV DNA was found using PCR in 12 normal breast specimens. This finding has raised the possibility of a therapeutic strategy for EBV positive breast cancers. Our approach to developing such a therapy would initially

involve investigation of EBV sequences in breast cancer cell lines and specimens, determination of whether treatment with Arginine Butyrate will induce the viral *TK* gene, determination *in vitro* of whether the induction of the *TK* gene and gene product makes the breast cancer cells now susceptible to GCV, and enrollment patients with breast carcinoma into the FDA-approved EBV-associated malignancy protocol and determination of their responses.

We have recently developed a virus-directed strategy for treating (EBV)-associated malignancies: Hodgkin's Disease, African Burkitt's lymphoma, certain Non-Hodgkin's lymphomas, and B cell lymphoproliferative disorders (EBV-LPD). This strategy is based on induction of the EBV thymidine kinase (TK) gene in latently-infected tumor cells employing the experimental drug Arginine Butyrate. After induction of the viral TK gene by Arginine Butyrate, addition of the FDA-approved nucleoside anti-viral agent ganciclovir (GCV) then leads to specific killing of virus-infected tumor cells which express the viral TK and spares normal cells. This potential therapy does not depend on the associated EBV genome being causally-related to the breast tumor. Just the presence of the EBV genome in latent form would be predicted to make the breast tumor susceptible to this combination protocol. The purpose of this proposal is to explore the association of EBV-infection and breast cancer, and to develop an EBV-based strategy for treating breast cancer.

This Progress Report describes the work performed in year 3, and summarizes work from years 1 and 2.

6. Body

Task 1: Refine molecular techniques to determine the presence of the Epstein-Barr virus genome in breast cancer biopsy specimens. This technology is readily available for lymphoid malignancies but needs to be tested for its applicability in epithelial-type tumors like breast cancer. **(completed)**

There are two pathology laboratory techniques in place in our hospital for detection of EBV in breast cancer specimens. The first is detection of EBERs, and the second is staining for LMP. We have tested two types of epithelial tumors for the presence of EBERs and for LMP, including HIV-associated lymphoepthelioma, nasopharyngeal carcinoma, and breast cancer. Both of these techniques detect the presence of EBV proteins in both the lymphoepthelioma and the nasopharyngeal carcinomas, and both of these tumors are causally-associated with EBV. Therefore, these techniques will detect EBV in epithelial cells. Neither standard technique has detected EBV proteins in two breast cancer cell lines which we know harbor the EBV genome. This is in agreement with a recent report by others (Glaser, 1998). This appears due to lack of expression of these viral genes in breast epithelial cells. We believed that the "gold standard" test for the presence of EBV, *in situ* DNA analysis, would be positive in cells harboring EBV, but it is not practical to screen breast tumors for EBV in a prospective way (Chu, 1998). A very recent publication

(Magrath, 1999; Bonnet, 1999) suggests that even *in situ* hybridization (ISH) underestimates the frequency of EBV clonal integration in breast cancers, and recommends PCR and RT-PCR. However, unless more widely-accessible pathology laboratory tests for EBV can be employed, it may be very difficult to prospectively identify patients who might be eligible for our EBV-TK induction therapeutic strategy.

We have, however, adapted a new, non-invasive method for monitoring response in patients with EBV-positive tumors (Stevens, 1999).

Task 2: Establish dose-response curves for induction of thymidine kinase transcript and protein in Epstein-Barr virus-containing tumors. **(completed in year 2)**

Dose-response curves for induction of TK have been performed in 10 tumor cell lines *in vitro*, to date. Concentrations of 0.1 mM butyrate are insufficient for induction in all tumors. The threshold for induction in both epithelial and lymphoid cultures is 0.5 mM. 1-2 mM induced viral TK maximally in 8/10 tumor cell lines. In the two cell lines in which TK induction did not occur at that concentration, no further increase in butyrate concentrations (up to 10 mM) resulted in any induction. There was no obvious reason for the failure of butyrate to induce TK in the two resistant cell lines, although it was noted that these lines similarly did not growth arrest in response to butyrate. This observation prompted an analysis of the molecular mechanisms underlying cell arrest by butyrate, and the second messengers and coupling of cell cycle and TK gene transcription (discussed in the Progress Report for year 2, and in Vaziri, 1998).

As proposed, we also studied TK induction in cells with newly-established latent-infections. Two such cells, JY and SPP, were studied. The dose-response for TK induction was identical to that described above. The time course for the induction, however, was quite different (discussed below, Task 3).

The magnitude of TK transcript induction was quite different between the tumor cell lines and the cells with newly-established latent infections. The average TK induction in the EBV-associated tumor cells was 5.6, with a range of 4-11. The average TK induction in the newly-latent cells was 2.3, with a range of 2-4.

TK protein levels follow mRNA levels in dose-response analysis, with, for example, 5-fold induction in RNA paralleling 5-fold induction of protein as assayed by immunoblot.

Summary of Evaluation of GCV and GCV + Arginine Butyrate on Lymphoma Cell lines

We demonstrated that: **1**) an mRNA transcript encoding the EBV-TK is induced in EBV(+) Burkitt's lymphomas, as well as in "tightly latent" B-cell Large Cell Lymphoma (LCL)

cell lines, following 12 h of incubation with 1 mM arginine butyrate; **2**) Induction of EBV-TK mRNA in an EBV(+) producer LCL was as efficient with Arginine Butyrate at 1 mM as it was with PMA (PMA has previously been the most potent known inducer of EBV-TK induction); **3**) We have achieved ~1 mM plasma levels of butyrate without adverse effects in Phase I studies using Arginine Butyrate as single agent therapy for refractory malignancies (Sanders, et al, 1995); **4**) We showed that Arginine Butyrate plus GCV caused synergistic toxicity in EBV-transformed and EBV-infected cells. The cells or cell lines were cultivated in the presence or absence of non-toxic doses of Butyrate (0.5 mM) or GCV (5 μM), or the combination of Arginine Butyrate plus GCV (see, for example, **Fig. 2.1**, *Appendix*). Because of TK induction, these cells were killed efficiently at the nontoxic doses of the individual drugs (0.5 mM Arginine Butyrate and 5 μM GCV). The combination was clearly much more toxic than either agent alone. EBV(-) cells co-incubated with butyrate and GCV at non-toxic doses were unaffected (not shown); **5**) We showed that the synergistic toxicity was dependent upon induction of the EBV-TK gene; **6**) When cell lines were co-incubated with butyrate and GCV, the toxic effects resulting from TK induction could easily be assessed even after the butyrate was washed out (**Fig. 2.2**).

Task 3: Establish time courses of viral *thymidine kinase* gene induction by Arginine Butyrate, and its half-life after induction. **(completed in year 2)**

Time courses for induction of TK have been performed in 10 EBV-latent cell lines *in vitro*, to date, with more careful analysis carried out in 5 tumors and 1 newly-latent cell line. 1 or 2 mM butyrate was used to induced viral TK.

In the tumor cells, maximal induction did not occur until 24 hr, with no or minimal induction observed at 6 and 18 hrs. Maximum levels persisted at 48 hrs, the latest time-point studied.

As proposed, we also studied the time-course of TK induction in cells with newly-established latent-infections. The time-course for TK induction was quite different than that was observed for the tumors. In the newly-latent cells, maximal induction occurred at 6 hr (the earliest time point studied, with levels falling at 12 hours and baseline levels at 24 hrs, despite persistent exposure to the drug. Washout studies showed that a 24 hr drug-free interval was necessary for the cells to again become susceptible to TK induction by butyrate.

These same time-courses and differences were found when phorbol ester (PMA) was used instead of butyrate as the TK-inducing agent.

In more recent studies, in lymphoid cells, EBV-TK induction by butyrate (and by PMA) is also transient, peaking at 6 hr, and returning to baseline by 24-48 hr, despite the continued presence of the drug (**Fig. 3.1**, *Appendix*).

In theory, this transient response might suggest that continuous administration of Arginine Butyrate may not be necessary. Rather, administration over 6-8 hr (*e.g.*, in an outpatient setting), might be sufficient, or even more efficient. (However, we must measure

the kinetics of TK protein and enzymatic activity induction by Butyrate in patients' tumor specimens, including the ability to re-induce expression of the enzyme, before consideration of any modifications of the current dosing regimen.)

Task 4: Analysis of *cis*-acting elements on viral TK promoter responsive to Arginine Butyrate. **(in progress)**

Is EBV-TK gene induction by Butyrate dependent upon cell cycle arrest? As discussed below, and detailed in Vaziri, et al., 1998, butyrate is a potent inducer of cell cycle arrest in G_1 phase. Because the latent growth program of EBV is linked to the cell cycle, we asked if we could dissociate cell cycle arrest from EBV-TK induction. Isobutyramide, an butyrate-derivative we previously developed [Perrine and Faller, 1994], is as potent as butyrate at induction of EBV-TK (**Fig. 4.1**). However, Isobutyramide does not induce G_1 arrest (**Fig. 4.2**), and therefore these two effects are distinct.

Define the molecular activity of the Butyrate compounds on cell growth and programmed cell death. Butyrate is a potent and reversible late G_1 blocker of the cell cycle. While this butyrate-induced G_1 arrest is reversible in normal cells, we and others have demonstrated that many transformed cells undergo apoptosis under the same conditions. [Please NOTE that this anti-tumor effect of butyrate as a single agent does **not** account for the positive clinical results we have observed in the butyrate+GCV combination. Using patient derived specimens and EBV-LCL lines, we have shown anti-tumor activity of the drugs in combination at doses where the individual agents alone have no cytotoxic activity (see Mentzer, et al.,1998).] Butyrate induces markedly increased levels of nuclear p53 protein. A causative role of p53 in mediating butyrate-induced cell cycle arrest was investigated in three ways: 1) Human cell lines lacking p53 were examined after butyrate treatment, and no compromise of G_1 arrest was observed; 2) Cells with an intact p53 were transfected with a mutant, dominant suppressor of p53. Both wild-type cells and cells expressing the dominant-negative p53 exhibited identical dose-dependencies for growth inhibition in response to butyrate; 3) Primary cultures of cells from p53 -/- 'knockout' mice were as susceptible as p53 +/+ cells to arrest in G_1 by butyrate. Therefore, G_1 growth arrest in response to butyrate occurs independently of p53. *p21* and *mdm-2* proto-oncogene transcripts, both of which can be transcriptionally-regulated by p53, were induced by butyrate at time points corresponding to growth arrest and accumulation of nuclear p53. However, induction of $p21^{Waf/Cip}$ by butyrate was found to be p53-independent, so $p21^{Waf/Cip}$ is not required for butyrate-induced cell cycle arrest.

We have identified inhibition of cyclin D_1 expression as a potential mechanism for butyrate-induced growth arrest. Butyrate inhibited mitogen-induced accumulation of cyclin D_1 transcripts in 3T3 cells as well as in mouse embryo fibroblasts from p21+/+ and p21-/- mice, and inhibited cyclin D expression and G_1 progression with similar dose-dependencies. Butyrate also perturbed G_1 signaling events distal to cyclin D expression, including mitogen-dependent phosphorylation of pRb. Butyrate inhibition of Rb

phosphorylation was sufficient to perturb downstream E2F-dependent events, including serum-induced cyclin E promoter-driven luciferase activity. The serum-dependent expression of both cyclins A and E was prevented by butyrate, concomitantly with inhibition of pRb phosphorylation. Loss of the normal Rb-mediated checkpoints induced by ectopic expression of the Human Papilloma Virus (HPV) E7 protein produced resistance to Butyrate-induced G_1 arrest. These data show that functional inactivation of pRb (and other pocket proteins), but not of p53, results in decreased sensitivity to the cytostatic actions of butyrate. Thus, butyrate-induced G_1 arrest in normal cells results in large part from a p53/p21-independent perturbation of the Rb signaling axis [Vaziri, 1998].

Is EBV-TK gene induction by butyrate dependent upon activation of the viral lytic program?

Butyrate and PMA have been shown to induce the EBV lytic cycle (albeit very weakly) in some latently-infected cells (see Protocol for references). To determine if activation of the lytic phase is required, we tested butyrate, isobutyramide, PMA and a number of fourth-generation, orally-bioavailable compounds (see section 3, below) for effects on induction of EBV "immediate-early" (BLZF1, BRLF1) and "late" (BALF4, BXLF2) genes, as markers of lytic cycle induction. We had already determined that a number of these new compounds are efficient at inducing EBV-TK mRNA (**Fig. 4.3**; see Torkelson, 1996 and Boosalis, 1998, for the structure/pharmacokinetics of these new oral agents). We found that induction of TK (**Fig. 4.5**), was associated with induction of the immediate-early genes (**Fig. 4.6**), and also of the late lytic genes (**Fig. 4.7**), suggesting that induction of the *TK* gene was the consequence of activation of an (abortive) lytic program, rather than direct activation of TK gene transcription.

Is TK gene induction by butyrate mediated by PKC or Histone Deacetylase?

Although we have extensive experience in analyzing butyrate-inducible promoters, a full exploration of the mechanisms by which Arginine Butyrate induces EBV-TK was beyond the scope of this translational grant. However, a few directed mechanisms were explored. Both PMA and bryostatin-1 induction of EBV-*TK* are thought to be mediated *via* activation of cellular PKC. Butyrate has been shown to activate certain cellular serine kinases, such as PKA and CKII. We used specific inhibitors of PKC to determine the role, if any, of PKC and (in particular PKC α, ε and β isozymes) in TK induction. Although the PKA agonist PMA induced TK expression in some EBV(+) cell lines, it did not do so in every cell line, whereas butyrate did invariably induce the gene. Furthermore, PKC inhibitors including staurosporine analogues, methyl-rac-glycerol and chelerythrin did not prevent TK induction by butyrates, suggesting that this induction is PKC independent.

We used trichostatin A and other selective HDAC inhibitors to determine if inhibition of HDAC resulted in regulation of the *TK* gene. TK was induced by TsA as efficiently as it was by butyrate. We also used the newer butyrate derivatives to determine if effects of these compounds on HDAC activity was associated with their effects on EBV-TK. KS-11, in particular, was a strong inhibitor of HDAC (**Fig. 4.4**). However, KS-11 did not induce TK

gene expression (**Fig. 4.5**). Therefore, the induction of *TK* by butyrates is not dependent upon HDAC inhibition.

Are Adhesion molecules on Breast Tumor Cells Modulated as a result of Butyrate Therapy?

Hematogenic spread of breast tumor cells involves reversible interactions between adhesion receptors on lymphoid cells and their counterparts on vascular endothelium, surrounding tissues, and matrices, and closely resembles extravasation of lymphocytes and leukocytes to the sites of inflammation. Hypoxia is known to induce extravasation of lymphocytes and leukocytes during ischemic injury. Tumor hypoxia analogously increases the metastatic potential of malignant lymphoid cells. We have recently identified and characterized a new adhesion molecule, HAL-1/13 (Hypoxia-Activated Ligand-1/13), which mediates the increases in lymphocyte and neutrophil adhesion to endothelium under hypoxic conditions. We used expression-cloning to identify this molecule as the lupus antigen, and DNA-PK-associated nuclear protein, Ku80. The HAL-1/13/Ku80 antigen is found on the surface of breast carcinoma cells, as well as several leukemic and solid tumor cell lines, including T and B lymphomas, myeloid leukemias, neuroblastoma, and rhabdomyosarcoma (Ginis and Faller, 1999, appended). Transfection and ectopic expression of (human) HAL-1/13/Ku80 on (murine) NIH-3T3 fibroblasts confers the ability of these normally non-adhesive cells to bind to a variety of human lymphoid cell lines, and this adhesion can be specifically blocked by HAL-1/13-neutralizing antibodies. Hypoxic exposure of breast carcinoma (MCF-7) cells, and lymphoma lines (Jurkat, JY), leukemia lines (U937), neuroblastoma (Kelly and SH-N-SK) lines resulted in upregulation of HAL-1/13/Ku80 expression at the cell surface, mediated by translocation of the antigen from the nucleus. This upregulation was coincident with an increased ability of the tumor cells to invade endothelial monolayers, and this invasion could be attenuated by anti-HAL-1/13 antibody. Hypoxia also potentiated lymphoid tumor cell transmigration through Matrigel filters. Anti-HAL-1/13 antibody inhibited this transmigration, and also the locomotion of hypoxic tumor cells on laminin. These studies indicate that the HAL-1/13/Ku80 molecule may mediate, in part, the increased invasiveness of tumor cells induced by hypoxia, as well as regulating hypoxia-induced adhesion of normal lymphocytes and leukocytes to endothelial cells.

In **summary**, we have dissociated cell cycle arrest from EBV-TK induction by butyrate. We have identified the molecular mechanism of action of butyrate in regulating the cell cycle [Vaziri, 1998]. We have demonstrated that the induction of TK by the butyrates is part of the activation of an abortive lytic cycle, and is not dependent upon PKC activity or upon HDAC inhibition.

Task 5: Enroll patients with Epstein-Barr virus-associated malignancies into the FDA-approved Phase I/II clinical trial. **(ongoing)**

The ongoing Phase I/II protocol will continue for at least another year, as we gather more efficacy and safety data for this drug combination, in a wider range of human malignancies

See **Table I** for current patient accrual and results.

Task 6: biochemical and molecular analysis of specimens obtained from patients with Epstein-Barr virus-associated malignancies, to determine the sensitivity of these tumors to Arginine Butyrate alone, to ganciclovir alone, and to the combination of drugs, and to correlate patient responses with *in vitro* sensitivity. (**Ongoing**)

As stated in the proposal, and required by the DOD Human Subjects approval, this Task is dependent on the unpredictable ability to obtain fresh tumor specimens suitable for culture prior to the initiation of the protocol, without putting the patient through additional surgical procedures. Although we have obtained pathology specimens of tumor tissue prior to treatment, and even obtained pathology specimens after treatment in 3 patients, we have still only obtained one tumor specimen which produced a tumor line in culture. The data described below on this cell line has been published (Mentzer, 1998), and described in the Progress Report for year 2) and will not be displayed herein unless requested.

The patient's peripheral blood mononuclear cells were grown in Dulbecco's Modified Eagle's Medium, ME) with 2,000 mg/L glucose (Sigma, St. Louis, MO), supplemented with 10% heat inactivated fetal calf serum (Sigma), 10 mM Hepes buffer, and 2 mM L-glutamine. With spontaneous growth of the cell line, the cells were passaged twice per week for more than eight months. The established cell line expressed a B lymphocyte phenotype identical to the primary tumor (kappa$^+$, CD19$^+$, CD20$^+$, CD21$^+$, CD23$^+$, CD30$^+$, CD40$^+$, and CD10$^-$). Southern blot analysis of the cell line demonstrated integrated genomic EBV DNA. These similarities between the established cell line and the primary tumor permitted use of the cell line in studies of arginine butyrate-induced *TK* expression.

The cell line was cultured with various concentrations of arginine butyrate, harvested at various time points, and studied for the induction of the *TK* transcript by RNA blot analysis. These studies demonstrated undetectable basal levels of the TK transcript, consistent with the latent state of viral replication of the EBV-associated cell line. In contrast, treatment of the cell line with arginine butyrate resulted in a dramatic induction of TK transcription within 12 hours.

Treatment of the established cell line with arginine butyrate alone and at concentrations ranging from 1 μM to 500 μM did not inhibit cell line proliferation. Similarly, treatment of the cell line with ganciclovir alone at concentrations up to 30 μM did not inhibit proliferation. In contrast, the combination of arginine butyrate at 500 μM plus ganciclovir at

10 and 30 μM synergistically inhibited cell proliferation measured by increases in fluorescence [RFU = relative fluorescent units] of the cytoplasmic label calcein. Assays of cell viability demonstrated that ganciclovir at 10 μM, 30 μM and 100 μM showed synergy with arginine butyrate at 500 μM or 1000 μM in decreasing cell viability at days 3 and 6 as defined by nuclear labeling with membrane impermeant fluorescent dye. No differences between treatment groups were observed at day 1 (not shown). These effects on tumor cell proliferation and viability were observed at concentrations of arginine butyrate and ganciclovir anticipated to be achievable *in vivo*. This patient also had a complete response to the combination of Arginine Butyrate and GCV.

In Summary: Evaluation of GCV and GCV + Butyrate on Patient-Derived Tumor Specimens -- Tumor cells were grown from the peripheral blood of the first two EBV(+) tumor patients we treated, and we demonstrated synergistic toxicity of the drug combination in his EBV(+) LCL B-cells [Mentzer, 1998]. These patients responded well to Arginine Butyrate + GCV *in vivo*.

Task 7: Ongoing pharmacokinetic analysis of Arginine Butyrate in patients in the Phase I trials. **(ongoing, and will continue until Phase I/II trial is terminated)**
See also Task 9.

We are continuing to collect samples on treated patients and are analyzing formal pharmacokinetics on Arginine Butyrate in these patients treated with the combination protocol, and have registered this data with the FDA in conjunction with our IND.

Task 8: Use *in vitro* data to modify and re-assess the Phase I clinical trial protocol. **(ongoing, and will continue until Phase I/II trial is terminated)**

None of the *in vitro* data to date suggests that we need to substantially modify our Phase I/II protocol. The profile of adverse events is quite favorable. The *in vitro* data on TK induction and time-course suggest that short courses of Arginine Butyrate may be insufficient for optimal induction (as detailed in the Progress Report for Year 1), and our current approach of sustained infusion may be optimal, or, at least, necessary. See also Task 9.

Task 9: Prepare and submit FDA report for Phase I trial completion. **(not initiated)**
Phase I/II trial is not yet complete. The ongoing Phase I/II protocol will continue for at least another year, as we gather more efficacy and safety data for this drug combination, in a wider range of human malignancies

Task 10: Prepare and submit the Phase II protocol for treatment of Epstein-Barr virus-positive breast malignancies to the FDA. Preparation includes a meeting with the FDA regarding the study and submission of IND. **(not initiated)**

This task was planned as part of a 5-year grant application. The grant was approved for only 3 years. The ongoing Phase I/II protocol will continue for at least another year, as we gather more efficacy and safety data for this drug combination, in a wider range of human malignancies, before establishing a pivotal Phase II trial.

Task 11: Analysis of other agents, including the oral agent Isobutyramide, for their effects on induction of thymidine kinase in EBV-positive tumor cells and sensitization to ganciclovir treatment. **(ongoing)**

Identify new, orally-bioavailable butyrate derivatives which induce EBV-TK expression. As we noted above, isobutyramide, an orally-bioavailable, long half-lived butyrate-derivative we have already developed through Phase I testing (IND #39,886), is as potent as butyrate at induction of EBV-*TK* (**Fig. 4.1**). We have also tested a number of fourth-generation, newly-synthesized, orally-bioavailable, β-oxidation-resistant compounds for effects on induction of EBV "early" genes. A number of these compounds are efficient at inducing EBV-*TK* mRNA (**Fig. 4.3**; see Torkelson, et al., 1996; and Boosalis, et al., 1997, for the structure/pharmacokinetics of these oral agents).

Isobutyramide, in particular has been studied in parallel with Arginine Butyrate in the extended induction and time course studies (**Tasks 2 and 3**), and also in cytotoxicity testing with GCV in the tumor cell lines (**Task 4**). Isobutyramide appears as efficient as Arginine Butyrate in induction of TK transcript. TK protein production has not yet been analyzed. Early cytotoxicity assays demonstrate synergistic killing with GCV. Unlike Arginine Butyrate, however, isobutyramide has no activity against breast cancer cell line by itself. We have identified several other derivatives / analogues of butyric acid, including dimethylbutyric acid (ST-20) and α-methyl-hydrocinnamic acid (ST-007), which induce TK, yet also have direct cytotoxic effects on breast carcinoma cell lines such as MCF-7 (**Fig. 11.1**).

In addition, we have developed more than 50 short-chain fatty acid derivatives which we tested for induction of globin genes [see Torkelson, 1996, Boosalis, 1997]. We have investigated this series of derivatives of short-chain fatty acids to determine: 1) what types of functional groups which could be substituted for a carbon and retain gene-inducing actions; and then, 2) what substitutions onto these types of structures prolong the half-life of the compound *in vivo*. Some substitutions, such as replacement of the carboxylic acid group with a tetrazole group, entirely abolished gene-inducing activity. Extending the carbon backbone beyond four carbons resulted in a loss of gene-inducing activity. However, a phenyl group could generally be used to replace a carbon without loss of this

activity. To confer resistance to β-oxidation and to β-glucuronidation, substitutions with dimethyl and other branched chain groups which result in steric hindrance to cleavage by the enzymes of oxidative metabolism and to create some resistance to renal excretion, and addition of halogens and phenoxy groups, have been effective. Current compounds of interest have 3-4 carbons and/or a phenyl group as backbone structure, such as cinnamic acid, propionic acid, or butyric acid, and have dimethyl, phenoxy, or halogen substitutions onto a phenyl ring. Some functional groups which typically delay metabolism but abolished gene induction were identified and discarded. We have also eliminated more than 30 second-generation gene-inducing compounds from further investigation because of undesirable metabolites, or limitations reported in the animal toxicology literature, or a significant obstacle in formulating them for human use.

Three classes of compounds which are of particular interest include phenoxy derivatives of acetic or propionic acid, the cinnamic acids, and dimethyl derivatives of fatty acids -- these families of compounds appear to have the biologic properties required of an improved TK-gene-inducing therapeutic. Three lead compounds, methylhydrocinnamic acid, phenoxyacetic acid, and dimethylbutyric acid strongly induce gene transcription and are not toxic even in very delicate hematopoietic cultures. These will be tested for activity in inducing EBV-TK to determine if they might offer a potential pharmacologic advantage over isobutyramide or Arginine Butyrate (*e.g.*, higher induction of TK, longer half-life of effect, or better dose-effect, etc.) In addition, some animal and human safety data for certain of these new compounds has already been obtained.

Task 12: Formal preclinical toxicity testing of Isobutyramide, in preparation for IND submission. **(completed)**

Two species 28-day toxicology (in beagle dog and rat) is complete. Metabolism and distribution studies are complete. Mutagenicity testing is complete. Results have been registered with the FDA (IND 39,886). Stability studies of the solution demonstrate >99% stability at 2 months at room temperature (IND 39,886).

Task 13: (months 34-36): Submission of IND for the combination of Isobutyramide and ganciclovir in the treatment of Epstein-Barr virus-associated breast cancer. **(not to be initiated at this time)**

This IND will not be initiated at present. The results using the IV preparation (Arginine Butyrate) have been very favorable in a group of patients with very advanced disease. The disadvantages of an IV drug in this setting are outweighed by the favorable results. It is not justified to switch to a clinically unproven TK-inducing agent, like Isobutyramide, simply for the purpose of convenience, and run the risk of less efficacy. If Arginine Butyrate plus GCV becomes first-line therapy for EBV-associated breast cancers,

we will consider testing isobutyramide in this setting, as convenience of delivery and half-life of the drug may become more of an issue in this setting.

7. Key Research Accomplishments:

- Developed, submitted, and initiated a FDA-registered Phase I/II clinical trial of Arginine Butyrate + GCV for the treatment of EBV-associated tumors.
- GMP-manufacture of Arginine Butyrate, preclinical toxicology, stability and Q/C.
- Evaluated of GCV + Butyrate on patient-derived tumor specimens
- Identified the mechanisms of action of Butyrate on induction of EBV TK expression
- Ten patients with EBV(+) tumors have been enrolled on the trial to date, with a number of other patients currently being evaluated for enrollment now.
- The trial is open at several major medical centers in addition to Boston University Medical Center
- We have added certain physicians to our IND, including Sloan-Kettering (Drs. R. O'Reilly and T. Small), Brigham and Women's (Dr. S. Mentzer), Dana-Farber (Dr. J. Fingeroth), Boston Children's (Dr. S. Burchett), Yale University (Dr. A. Levy) and Hospital Necker, Paris (Dr. O. Hermine).
- Identified new, orally-bioavailable butyrate derivatives which induce EBV-TK expression.
- Preclinical toxicology of Isobutyramide (oral agent) completed. Two species 28-day toxicology (in beagle dog and rat) is complete. Metabolism and distribution studies are complete. Mutagenicity testing is complete. Results have been registered with the FDA (IND 39,886). Stability studies of the solution demonstrate >99% stability at 2 months at room temperature (IND 39,886).

8. Reportable Outcomes

Publications:

Original Reports:

Mentzer, S.J., Fingeroth, J., Reilly, J.J., Perrine, S.P., and Faller, D.V. Arginine Butyrate-induced susceptibility to ganciclovir in an Epstein-Barr Virus (EBV)-associated lymphoma. *Blood Cells Molecules.Dis.* 24:114-123, 1998

Vaziri, C., Stice, L.L., and Faller, D.V. Butyrate-induced G1 arrest results from p21-independent disruption of retinoblastoma-mediated signals. *Cell Growth Differ.* 9:465-474, 1998.

Ginis I and Faller, DV. Hypoxia Affects Tumor Cell Invasiveness *In Vitro*: The Role of

Hypoxia-Activated Ligand HAL1/13 (Ku 86 autoantigen)., 1999, *submitted for publication.*

Abstracts:

1. THE HYPOXIA-ACTIVATED LIGAND HAL-1/13 IS IDENTICAL TO Ku80, AND MEDIATES LYMPHOID CELL ADHESION AND TUMOR CELL INVASIVENESS IN VITRO. I. Ginis,* E. Lynch,* and D.V. Faller. Cancer Research Center, Boston University School of Medicine, Boston, MA American Society of Hematology Annual Meeting, 1999.

2. TREATMENT OF EPSTEIN-BARR VIRUS (EBV)-ASSOCIATED LYMPHOMAS AND PTLD USING ARGININE BUTYRATE TO INDUCE VIRAL *TK* GENE EXPRESSION: INITIAL FINDINGS OF A PHASE I/II TRIAL. D.V. Faller, O. Hermine,* T. Small, R. O'Reilly, J. Fingeroth,* S.J. Mentzer,* and S.P. Perrine. Cancer Research Center, Boston University School of Medicine, and Brigham and Women's Hospital, Boston, MA; Hospital Necker, Paris, France; Memorial-Sloan Kettering, New York, N.Y. American Society of Hematology Annual Meeting, 1999.

9. Conclusions

In the 36 months of research under this grant, we have completed the majority of the Tasks we had set for months 1-36 (Tasks 1, 2, and 3, although we will continue to study mechanisms of resistance of TK induction). The new data we generated concerning molecular mechanisms of butyrate action on gene expression completed Task 4. We have enrolled several new patients onto the clinical protocol, with pharmacokinetic studies collected, safety assessed, and responses noted (Tasks 4-7).

The development of the first new, orally-bioavailable form of TK-gene regulating agents is complete (Tasks 11 and 12), although the success of our protocol to date obviates the need to begin a study with an oral agent (Task 13).

Because we received only 3 years of funding instead of 5 years, we have not yet completed our Phase I/II protocol. Accordingly, we have not yet registered a new Phase II trial. Indeed, because of the favorable responses to our original protocol, we have not found the need to alter our original protocol (Tasks 8, 9, 10).

SUMMARY of Clinical Progress: We established contract GMP manufacture of our experimental drug. We have designed, FDA-registered, and instituted a Phase I/II trial based on our preclinical data and working hypothesis. The trial is now ongoing at multiple clinical cancer centers across the country and in Europe. Remarkable clinical responses have been observed in the majority of the (small number of) patients treated. We are now FDA-approved to enroll pediatric patients, and this experimental therapy is FDA-approved

as first-line treatment of EBV(+) tumors.

DETAILS of Clinical Progress: During this period of DOD funding, we developed, submitted, and initiated a FDA-registered Phase I/II clinical trial of Arginine Butyrate + GCV for the treatment of EBV-associated tumors. This project required GMP-manufacture of Arginine Butyrate, preclinical toxicology, stability and Q/C. Ten patients with EBV(+) tumors have been enrolled on the trial to date, with a number of other patients currently being evaluated for enrollment now. The trial is open at several major medical centers in addition to Boston University Medical Center and added certain physicians to our IND, including Sloan-Kettering (Drs. R. O'Reilly and T. Small), Brigham and Women's (Dr. S. Mentzer), Dana-Farber (Dr. J. Fingeroth), Boston Children's (Dr. S. Burchett), Yale University (Dr. A. Levy) and Hospital Necker, Paris (Dr. O. Hermine). (A number of other institutions have asked to open this trial, but our current financial resources have precluded this.)

All of the patients studied had been heavily pre-treated with conventional therapies, including chemotherapy, radiotherapy, immunotherapy, and sometimes bone marrow transplantation, with no response, prior to beginning our protocol (**Table I**, *Appendix*). Four of the eight patients have had complete responses to a single cycle of therapy (although several of these patients ultimately succumbed to complications of their underlying immunodeficiency). We now have several long-term (>3 years) survivors of these otherwise invariably lethal tumors. One patient, listed here as a partial-responder, had only 5 days of therapy, but hepatic enlargement of unknown etiology caused us to take him off protocol while it was being investigated. One patient with tumor that was positive in only one lymph node for EBV, but negative in the primary tumor, completed the 21-day cycle uneventfully, but did not respond. There have been no significant side effects that we have been definitely able to ascribe to the drug combination, although one patient demonstrated reversible lethargy/somnolence at 1500 mg/kg/day, two patients complained of anorexia or grade 2 nausea, and one patient suffered fulminant acute liver failure off of the drug, after rapid and complete resolution of her tumor. These potential adverse reactions have been reported to the FDA.

We have been able to culture tumor cells from the two patients treated in Boston, (Mentzer, 1998), and have demonstrated synergistic susceptibility to the drug combination in these primary tumor cells.

On the basis of the clinical responses and lack of serious toxicity, we have, over the last year, been allowed by the FDA to: 1) Apply this novel treatment as first-line therapy for EBV(+) tumors. Prior treatment with chemotherapy, etc. is not required before our protocol can be instituted; 2) Enroll children 5 years and older on this protocol. This is an unusual step for the FDA to take, and reflects their confidence in our approach, as well as the lack of other effective therapies; 3) Enroll HIV(+) patients. We excluded HIV(+) patients initially because of theoretical concerns about effects of Arginine Butyrate on viral replication. The ability to measure HIV viral titers serially, the advent of triple-drug anti-HIV therapy, and the lack of any other effective therapies, have led the FDA to approve enrollment of HIV(+) patients with EBV(+) tumors.

10. References

Bonnet M, JM Guinebretiere, E Kremmer, V Grunewald, E Benhamou, G Contesso, I Joab. Detection of Epstein-Barr virus in invasive breast cancers. *Journal of the National Cancer Institute*, 1999, 91:1376-1381

Chu, J.S., Chen, C.C., and Chang, K.J. In situ detection of Epstein-Barr virus in breast cancer. *Cancer Lett.* 124:53-57, 1998. 304-3835.

Ginis I and Faller, DV. Hypoxia Affects Tumor Cell Invasiveness *In Vitro*: The Role of Hypoxia-Activated Ligand HAL1/13 (Ku 86 autoantigen)., 1999, *submitted for publication.*

Glaser, S.L., Ambinder, R.F., DiGiuseppe, J.A., Horn-Ross, P.L., and Hsu, J.L. Absence of Epstein-Barr virus EBER-1 transcripts in an epidemiologically diverse group of breast cancers. *Int.J.Cancer* 75:555-558, 1998. 20-7136.

Lallemand, F., Courilleau, D., Sabbah, M., Redeuilh, G., and Mester, J. Direct inhibition of the expression of cyclin D1 gene by sodium butyrate. *Biochem. Biophys. Res. Com.* 229: 163-169, 1996.

Magrath, I, Bhatia, K. Breast cancer: a new Epstein-Barr virus-associated disease? *Journal of the National Cancer Institute*, 1999, 91:1349-1350.

Mentzer, S.J., Fingeroth, J., Reilly, J.J., Perrine, S.P., and Faller, D.V. Arginine Butyrate-induced susceptibility to ganciclovir in an Epstein-Barr Virus (EBV)-associated lymphoma. *Blood Cells Molecules.Dis.* 24:114-123, 1998

Nakano, K., Mizuno, T., Sowa, Y., Orita, T., Yoshino, T., Okuyama, Y., Fujita, T., Ohtani-Fujita, N., Matsukawa, Y., Tokino, T., Yamagishi, H., Oka, T., Nomura, H., and Sakai, T. Butyrate activates the WAF-1/CIP1 gene promoter through sp1 sites in a p53-negative colon cancer cell line. *J. Biol. Chem.* 272: 22199-22206, 1997.

Siavoshian, S., Blottiere, H. M., Cherbut, C., and Galmiche, J. P. Butyrate stimulates cyclin D and p21 and inhibits cyclin-dependent kinase 2 expression in HT-29 colonic epithelial cells. *Biochem. Biophys. Res. Com.* 232: 169-172, 1997.

Stevens SJC, MBHJ Vervoort, AJC vandenBrule, PL Meenhorst, CJLM Meijer, JM Middeldorp. Monitoring of Epstein-Barr virus DNA load in peripheral blood by quantitative competitive PCR. *Journal of Clinical Microbiology*, 1999, 37:2852-2857

Yoshida, M. and Beppu, T. Reversible arrest of proliferation of rat 3Y1 fibroblasts in

both the G1 and G2 phases by trichostatin A. *Exp. Cell Res.* 177: 122-131, 1988.

Vaziri, C., Stice, L.L., and Faller, D.V. Butyrate-induced G1 arrest results from p21-independent disruption of retinoblastoma-mediated signals. *Cell Growth Differ.* in press, 1998.

Wintersberger, E., Mudrak, I., and Wintersberger, U. Butyrate inhibits mouse fibroblasts at a control point in the G1 phase. *J. Cell. Biochem.* 21: 239-247, 1983.

8. Appendices

Table:	1
Figures:	11
Publications:	2
Meeting Abstracts:	2

Final Report Bibliography

TABLE I

Patient	Age	Site	EBV status	Prior Rx	Hospital	Butyrate+GCV Treatment	Response	Adverse Events
1	48	Thorax	(+)	Cx,XRT,IF	BWH	10 days	Complete	None
2	24	Brain	(+)	Cx,XRT,IF	DFCI	10 days	Complete	None
3	48	Nasal	(+)	Cx,XRT	Paris	21 days	Complete	Stupor
4	3	Diffuse	(+)	Cx,XRT,BMT	MSK	7 days	Partial	None
5	30	GI	(+)	Cx,XRT,IF	MSK	21 days	Complete	Lethargy
6	22	Diffuse	(+/-)	Cx,XRT,BMT	Yale-NH	21 days	None	Nausea
7	7	GI (HIV)	(+)	Ganciclovir	Childrens	21 days	Stable Dis.	Nausea
8	37	Diffuse (HIV)	(+)	Cx,XRT	Paris	21 days	Complete (Recurred)	None
9	46	Breast	(+)	Cx, XRT	DFCI	on-study	on-study	on-study
10	54	Thorax	(+)	CX x 2	PAris	on-study	on-study	on-study

Cx = Chemotherapy
XRT = Radiotherapy
IF = Interferon
BMT = Bone Marrow Transpl.

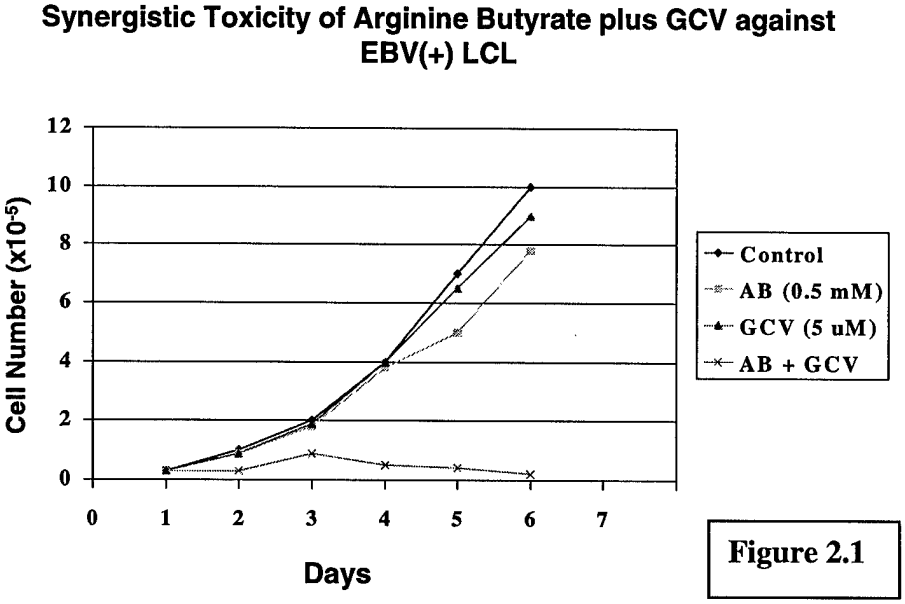

Figure 2.1

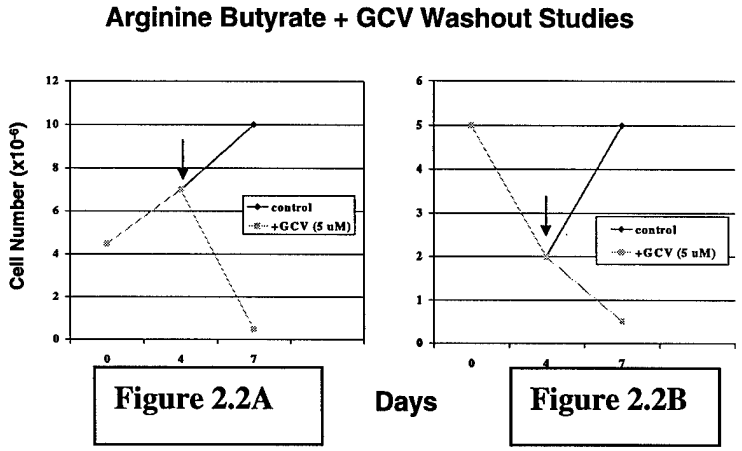

Figure 2.2A

Figure 2.2B

Figure 2.1: Growth curves of a latent EBV(+) LCL cell line grown in the presence of non-toxic doses of Arginine Butyrate (0.5 mM) or ganciclovir (GCV) (5 μM). The cells were also cultivated in the presence of the combination of Arginine Butyrate plus GCV. The combination was clearly much more toxic than either agent alone.

Figure 2.2: Significant synergy was seen in the combination of GCV and Arginine Butyrate on all LCL cell lines. An EBV(+) B-cell LCL that is latent was incubated in the presence of 0.5 mM Arginine Butyrate (non-toxic) (**A**), or 2.0 mM (cytotoxic) Arginine Butyrate (**B**) for 3 days, after which time butyrate was washed out and GCV added to some plates (+) at 5.0 μM. Because of TK induction, the cells were killed efficiently at the nontoxic doses of the individual drugs. EBV(-) cells coincubated with butyrate and then GCV at non-toxic doses were unaffected (not shown).

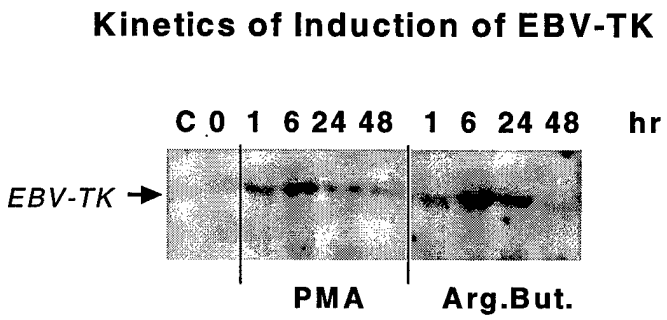

Figure 3.1

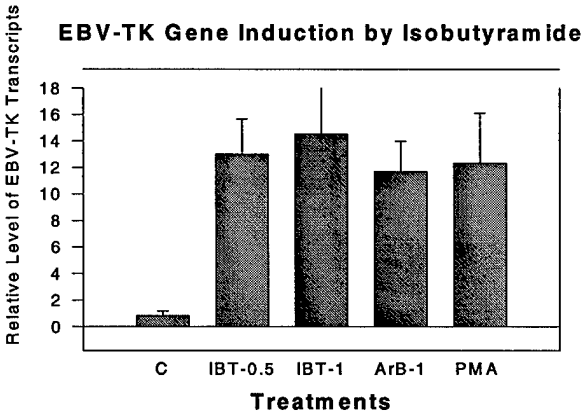

Figure 4.1

Figure 3.1: Blot hybridization of total RNA from the FF41 cell line, incubated with either PMA (20 ng/ml) or Arginine Butyrate (Arg. But.) (1 mM) for time periods shown. Blots were probed with the radiolabeled Bam HI X fragment of EBV containing the TK gene.

Figure 4.1: Induction of EBV-TK mRNA by Isobutyramide. Blot hybridization of total RNA from the FF41 (an LCL) cell line, incubated with either PMA (20 ng/ml), Arginine Butyrate at 1 mM (ArB-1), or Isobutyramide at 0.5 mM and 1 mM (IBT-0.5 and IBT-1) for 12 hrs. Autoradiograms of RNA blots were quantitated with an LKB laser densitometer (Pharmacia, Upsalla, Sweden), and the results plotted. EBV-TK mRNA levels expressed by untreated FF41 cells were arbitrarily set at 1. Induction of EBV-TK mRNA in this EBV(+) producer LCL was as efficient with Isobutyramide as it was with Arginine Butyrate or with PMA.

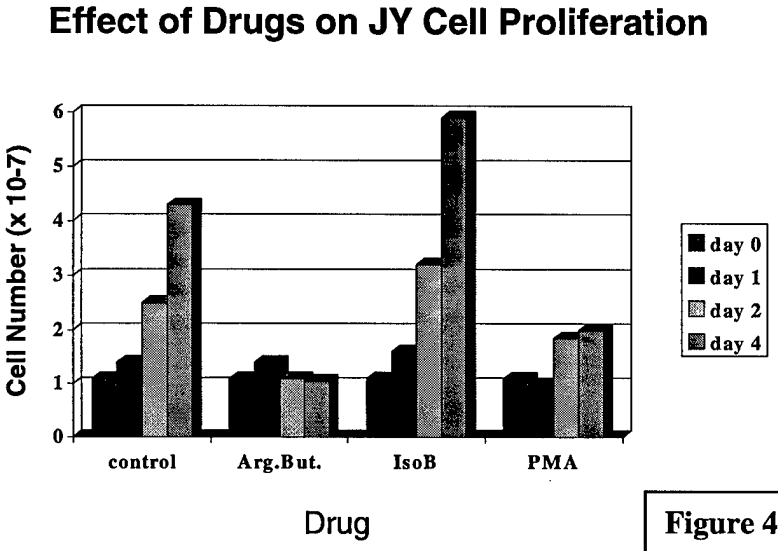

Figure 4.2

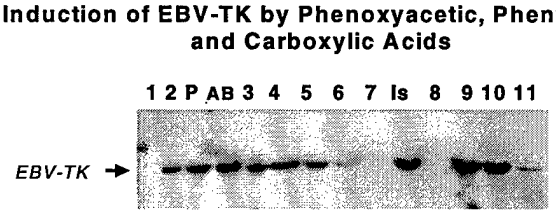

Figure 4.3

Figure 4.2: Effect of Pharmacologic inducers of EBV-TK on cell proliferation. JY cells (EBV-LCL) were cultured alone or with drugs at concentrations optimal for EBV-TK induction: Arginine Butyrate (1 mM), Isobutyramide (1 mM), or PMA (100 nM). Viable cells were quantitated at the time intervals indicated. All conditions were tested in quadruplicate.

Figure 4.3: Blot hybridization of total RNA isolated from the FF41 cell line, incubated with either PMA (P) at 20 ng/ml or Arginine Butyrate (AB) at 1 mM, or Isobutyramide (Is) at 1 mM, or a number of third and fourth generation, orally-bioavailable butyric acid derivatives (phenyalkyls: compounds 1-3; phenylacetics: compounds 4-7; carboxylics: compounds 8-11) for 12 hrs periods shown. Blots were probed with the radiolabeled Bam HI X fragment of EBV containing the TK gene.

Fig. 4.4 Induction of TK in P3HR1 cells by Butyrate, Butyrate analogues, and others

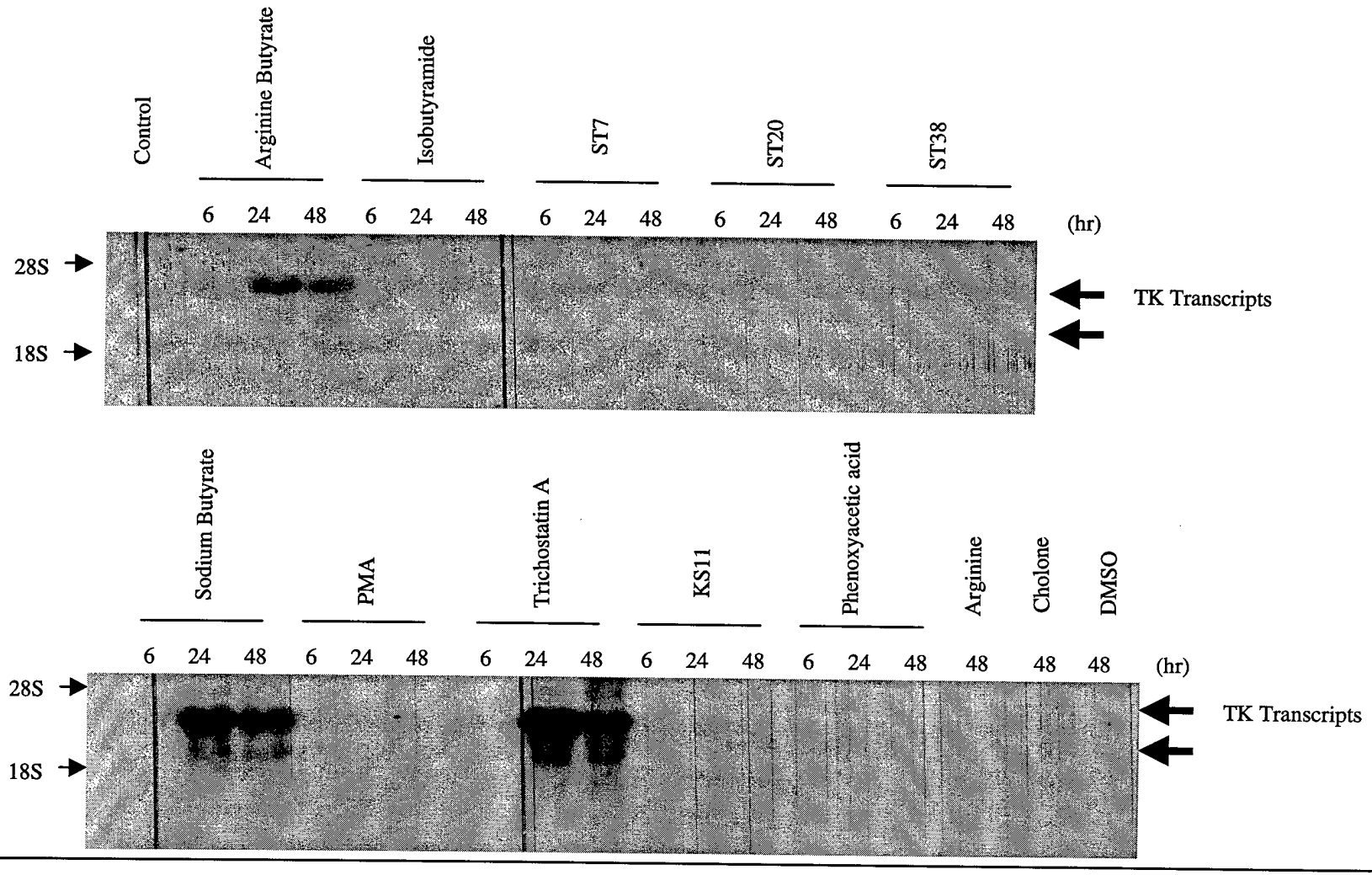

Fig. 4.5 ion of Zta and Rta in P3HR1 cells by Butyrate and Trichostatin A

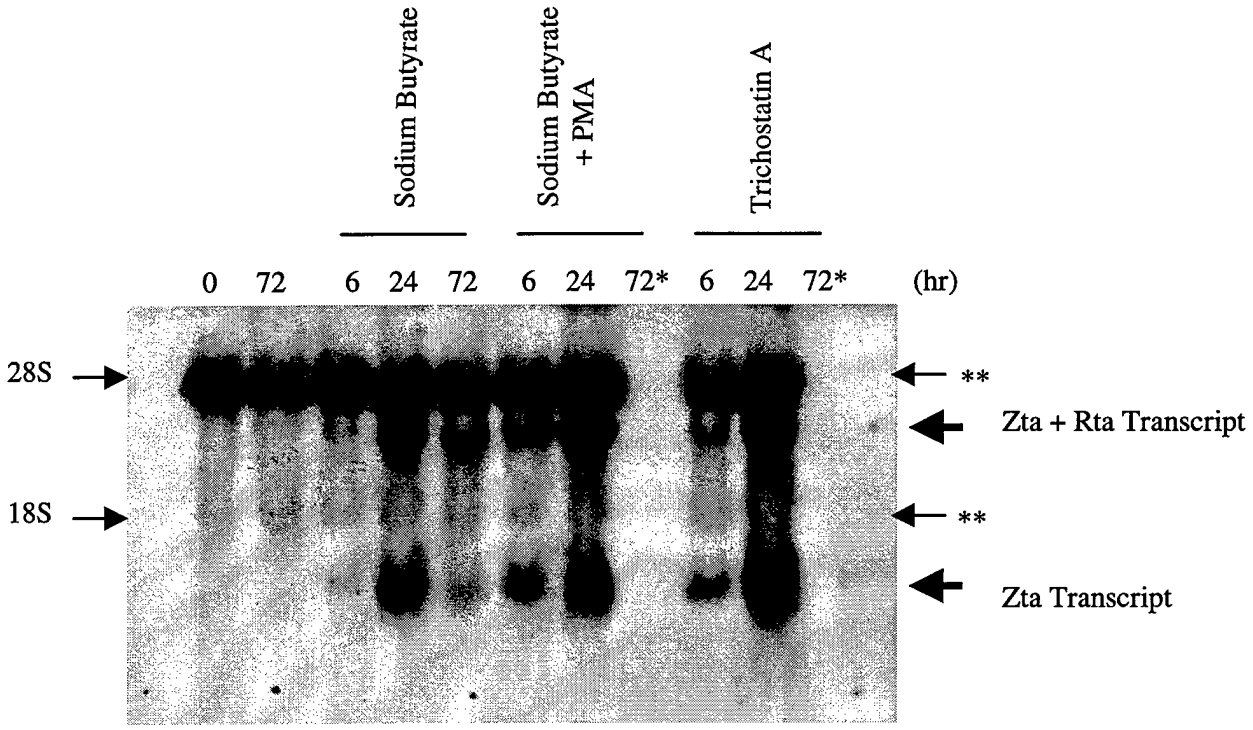

* Empty lane

** 28S and 18S background (Z Probe contains poly(A) tail)

Fig. 4.6 ›n of BALF4 (late gene, gp85) in P3HR1 cell by Butyrate and Trichostatin A

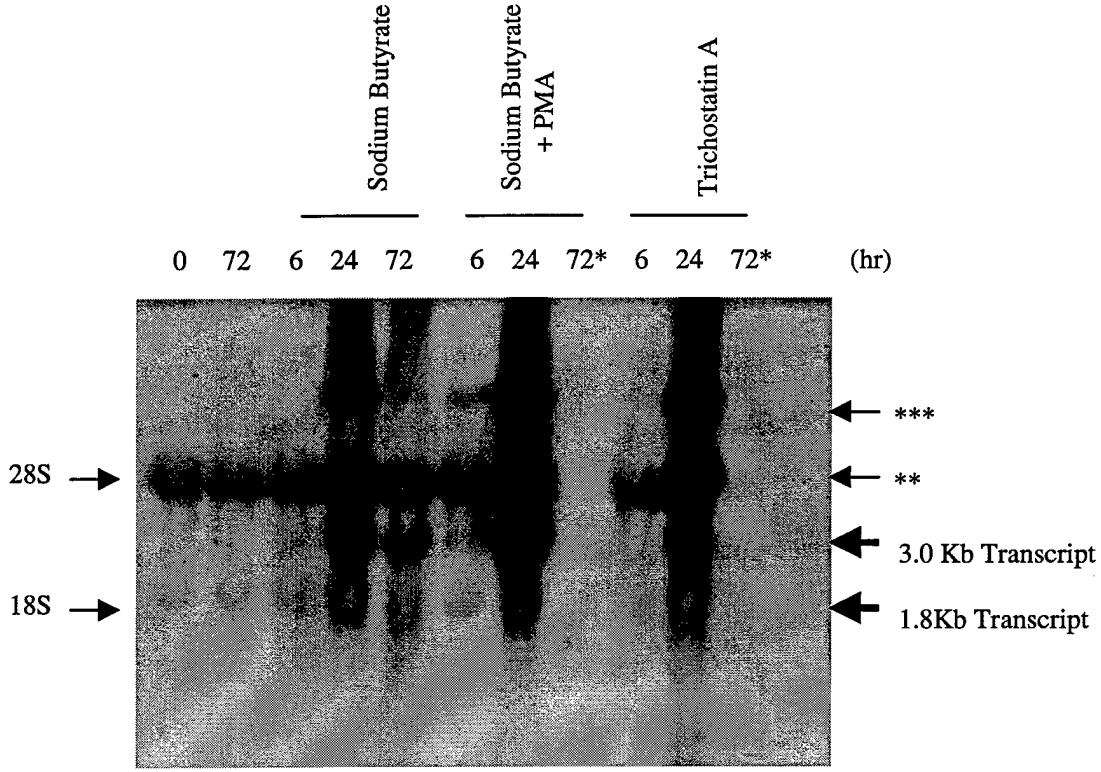

* Empty lane

** Non-specific binder

*** Unknown

Figure 4.4: Blot hybridization of total RNA isolated from the P3HR11 cell line, incubated with either PMA (P) at 20 ng/ml or Butyrate at 1 mM, or Isobutyramide (Is) at 1 mM, or Trichostatin A, or a number of third and fourth generation, orally-bioavailable butyric acid derivatives (ST7, 20, 38, PAA or KS11) for the time periods shown. Blots were probed with the radiolabeled Bam HI X fragment of EBV containing the TK gene.

Figure 4.5: Blot hybridization of total RNA isolated from the P3HR11 cell line, incubated with either PMA (P) at 20 ng/ml or Butyrate at 1 mM, or Trichostatin A for the time periods shown. Blots were probed with the radiolabeled fragment of EBV containing the ZTA and RTA genes.

Figure 4.6: Blot hybridization of total RNA isolated from the P3HR11 cell line, incubated with either PMA (P) at 20 ng/ml or Butyrate at 1 mM, Butyrate at 1 mM, or Trichostatin A for the time periods shown. Blots were probed with the radiolabeled fragment of EBV containing the BALF gene.

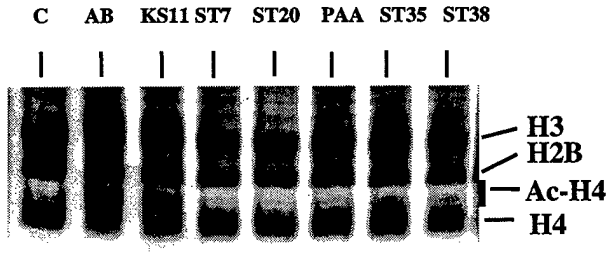

Figure 4.7

Figure 4.7: HDAC-inhibitory activity, or its absence, was tested in a panel of SCFAs. Cells were treated for 12 or 24 hours with growth-promoting or growth-inhibitory SCFAs at concentrations shown to be biologically active in culture, with Trichostatin A at 1 uM as a positive control for HDAC inhibition. Cells were left untreated as a negative control. Whereas growth-inhibitory compounds Arginine Butyrate (AB) and KS11) produced high levels of acetylated H4, other compounds (ST7, ST20, PAA, ST35 or ST38) did not have an effect on histone H4 acetylation.

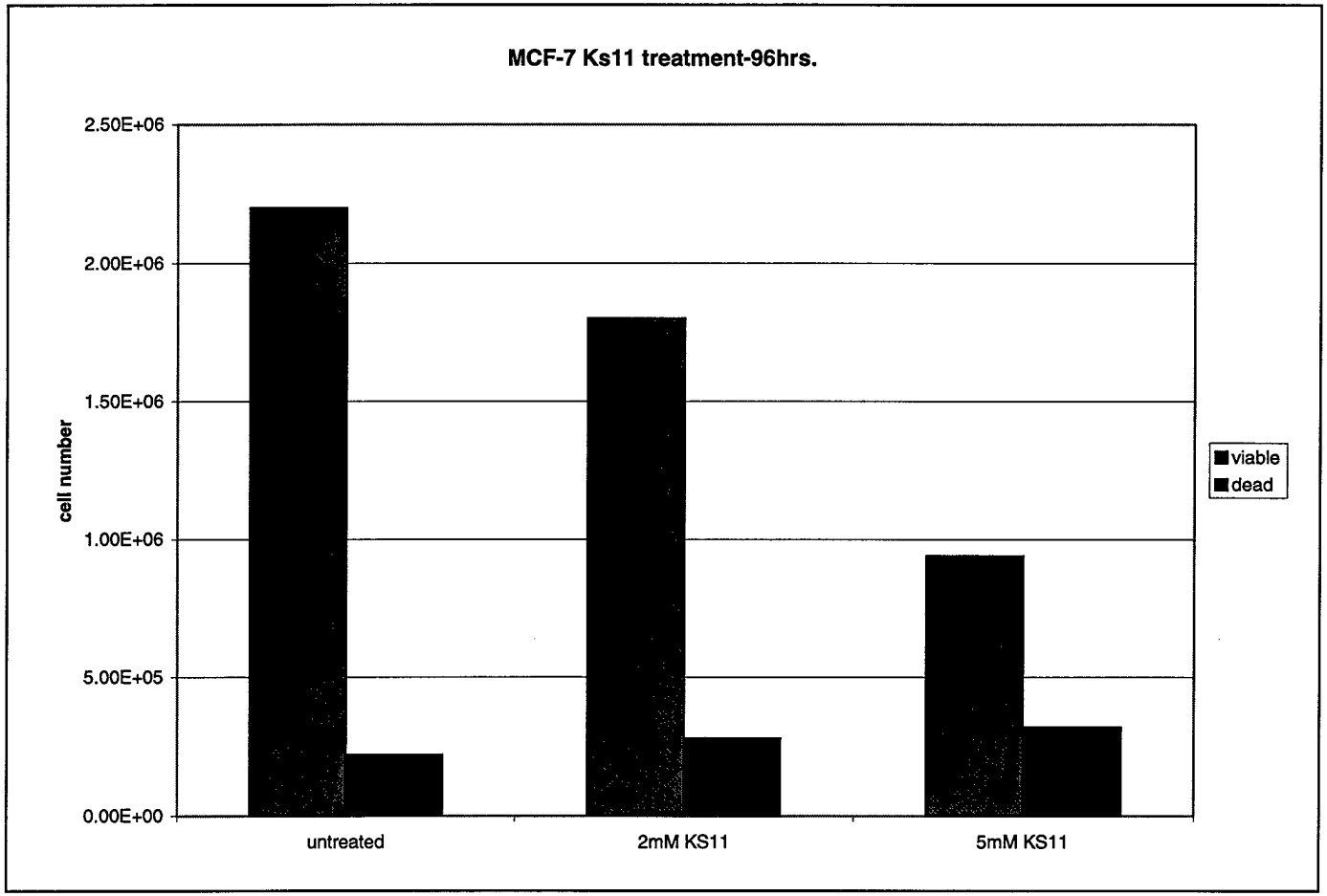

Figure 11.1: KS11 (at the concentrations shown) was used to treat MCF 7 cells for 24 hr. The viable and non-viable cells were enumerated, as assessed by trypan blue staining.

Butyrate-induced G_1 Arrest Results from p21-independent Disruption of Retinoblastoma Protein-mediated Signals[1]

Cyrus Vaziri, Ligaya Stice, and Douglas V. Faller[2]

Cancer Research Center, Boston University School of Medicine, Boston, Massachusetts 02118

Abstract

When treated with millimolar concentrations of butyrate, many cell types undergo growth arrest in the G_1 phase of the cell cycle. However, the molecular basis of butyrate-induced G_1 arrest has not been elucidated. We have investigated the molecular mechanisms of butyrate-induced G_1 arrest in synchronized cultures of untransformed 3T3 fibroblasts. We tested the hypothesis that butyrate-induced growth arrest might be mediated by the p21 cyclin-dependent kinase inhibitor. Sodium butyrate-treated 3T3 cells did, indeed, express elevated levels of p21 mRNA under conditions of G_1 arrest. Surprisingly, however, primary cultures of fibroblasts from transgenic p21 "knockout" (p21−/−) mice and fibroblasts from wild-type p21-proficient (p21+/+) mice underwent butyrate-induced G_1 arrest with similar dose dependencies. Therefore, p21 expression was not necessary for butyrate-induced G_1 arrest. To identify other potential mechanisms of butyrate-induced growth arrest, we analyzed the butyrate sensitivity of key mitogenic signaling events during G_1. We found that butyrate inhibited the mitogen-dependent transcriptional induction of cyclin D1 and phosphorylation of retinoblastoma (Rb), both in p21-proficient 3T3 cells and in p21+/+ and p21−/− mouse embryo fibroblasts. Butyrate treatment also prevented mitogen-dependent transcriptional induction of cyclin E and expression of cyclin A, cell cycle events that are temporally distal to expression of cyclin D and are necessary for entry into S phase. Abrogation of a requirement for cyclin D/cyclin-dependent kinase-dependent phosphorylation of Rb (by ectopic expression of the human papilloma virus E7 oncoprotein in 3T3 cells) resulted in decreased sensitivity to the antiproliferative actions of butyrate. Overall, these data show that butyrate-induced G_1 arrest is, in large part, independent of p21 induction. Instead, butyrate-induced growth arrest appears to result from perturbation of the Rb signaling axis at the level of or at a stage prior to cyclin D1 expression.

Introduction

Butyrate is a nontoxic short-chain fatty acid that is produced naturally during the microbial fermentation of dietary fiber in the colon (1). Millimolar concentrations of butyrate have been reported to cause a G_1 block, inhibition of cellular proliferation, and inhibition of onset of DNA synthesis in a large number of cultured cell types, including Chinese hamster ovary cells (2), adenovirus-infected and uninfected HeLa cells (3), 3T3 mouse fibroblasts (4), normal and SV40-transformed human keratinocytes (5), and normal and Rous sarcoma virus-transformed chicken heart mesenchymal cells (6). All of these reports are consistent with a butyrate-mediated cell cycle block, thought to be in the G_1 phase of the cell cycle (7). The butyrate cell cycle block is associated with a putative restriction point related to termination of expression of a labile protein (7, 8). However, the precise mechanisms of sodium butyrate-induced G_1 arrest have not been elucidated.

Butyrate resulting from colonic fermentation of dietary fiber may exert an antiproliferative effect upon the epithelial cells of the mucosal epithelium (9). Therefore, it has been proposed that naturally occurring dietary fiber-derived butyrate protects against cancer of the colon (9, 10). Due to their potent antiproliferative effects and lack of toxicity, butyrate compounds have also received some attention as potential cancer therapeutic agents. Understanding the mechanisms whereby butyrate inhibits cell cycle progression may enable identification of novel targets for therapies against cancer and, possibly, other proliferative disorders. This information could also provide new insight into normal mechanisms of cell growth control. Therefore, there is considerable interest in defining the mechanisms of butyrate-induced growth arrest.

Mitogen-stimulated progression through the replicative cell cycle is mediated by intracellular signal transduction events, involving generation of second messengers, activation of protein kinase cascades, and gene transcription (reviewed in Refs. 11–13). It is probable that butyrate-induced growth arrest results from modification or perturbation of these crucial mitogenic signaling events. Indeed, several investigators have demonstrated effects of butyrate on some of the mitogenic signaling events that are considered to be important for normal cell cycle progression.

However, despite reports of correlations between G_1 arrest and perturbation of certain mitogenic signaling events, there exists a certain amount of confusion in the literature regarding the nature of responses of specific signaling

Received 2/19/98; revised 5/5/98; accepted 5/5/98.

The costs of publication of this article were defrayed in part by the payment of page charges. This article must therefore be hereby marked *advertisement* in accordance with 18 U.S.C. Section 1734 solely to indicate this fact.

[1] Supported by the Department of Defense United States Army Breast Cancer Research Program (to D. V. F.) and by a Leukemia Society of America Translational Service Award (to D. V. F.). C. V. was funded by a postdoctoral fellowship from the American Cancer Society, Massachusetts Division Inc.

[2] To whom requests for reprints should be addressed, at Cancer Research Center, Boston University School of Medicine, 80 East Concord Street, Boston, MA 02118.

events to treatment with butyrate. For example, expression of cyclin D, a key regulator of G_1 progression, has been reported to be both induced (14) and suppressed (15) in response to sodium butyrate. Such discrepancies may result, in part, from the fact that many studies of butyrate action have been performed using tumor-derived cells. Transformed cell lines are inherently genetically unstable and are likely to have acquired numerous mutations, during both tumorigenesis and selection in culture. Potentially, such lesions could have profound effects on mitogenic signal transduction pathways, thereby resulting in idiosynchratic responses to butyrate.

We have attempted to resolve some of the controversy regarding molecular mechanisms of sodium butyrate-induced G_1 arrest. In experiments described here, we have tested the hypothesis that butyrate modifies mitogenic G_1 signaling pathways in the context of a nontransformed cell line with well-defined growth properties in culture. We chose to use mouse 3T3 fibroblasts for these studies because these nontransformed cells are stringently growth regulated and have well-defined growth factor requirements in culture (11). Moreover, much is known regarding the signal transduction events that mediate responses to positive and negative regulators of growth in these cells. Importantly, many of the findings relating to cell cycle regulation originally documented in 3T3 fibroblasts have since been shown to be applicable to many other cells in culture and *in vivo*. Indeed, results from numerous studies in 3T3 cells have provided a paradigm for mammalian cell cycle control (11). Cell cycle regulation as exemplified by 3T3 cells will be considered briefly below.

For exponential growth, 3T3 fibroblasts require exogenous growth factors, usually provided by the addition of 10% serum to the culture medium. However, upon transfer to medium containing low concentrations (0.5%) of serum, the cells exit the replicative cycle and undergo growth arrest (a state also termed "quiescence" or "G_0"). Upon readdition of 10% serum to growth-arrested fibroblasts, the cells synchronously reenter the cell cycle and, after a lag phase of ~12 h (termed "G_1"), begin to replicate their DNA. DNA synthesis (S phase) lasts ~6 h and is followed by another 5–6-h lag phase (G_2), which precedes mitosis. Following mitosis, cells return to the quiescent state or continue to cycle, depending upon culture conditions, such as cell contact, or on the local concentration of growth factors (11).

Purified fibroblast mitogens, such as PDGF[3] (which accounts for much of the mitogenic activity present in serum), are sufficient to stimulate quiescent cells through G_1 and into S phase. To progress through G_1 into S phase, cells require continuous stimulation by mitogen up until a point ~1 h prior to S phase (termed the "R"-point, probably equivalent to "START" in yeast). Upon reaching the R-point, the cells become committed to replicate their DNA, even in the absence of exogenously added growth factors. Therefore, G_1 is a critical "decision-making" time in which cells commit to enter S phase and replicate their genetic material or remain in a quiescent state (11). Some of the key molecular signals that influence this decision-making process are described below.

Binding of growth factors (such as PDGF) to appropriate cell surface receptors initiates a series of temporally ordered intracellular events, including activation of small G-proteins, generation of second messenger molecules, and stimulation of protein kinase cascades (11–13). These events result in the transcription of genes, the products of which enable cells to progress through G_1. Some of the critical signaling events that occur in late G_1 and are absolutely necessary for initiation of DNA replication are summarized as follows. Mitogen-induced cyclin D expression begins during mid-G_1 and results in activation of CDKs 4 and 6. Active CDK-cyclin D complexes phosphorylate the Rb tumor suppressor protein and also, most probably, other important substrates. Rb phosphorylation results in release of an inhibitory constraint (imposed by hypophosphorylated Rb) upon the E2F transcription factor. Transcriptionally active heterodimers of E2F and DP (E2F-related proteins) promote the expression of a subset of genes, including cyclin E. E2F induction of cyclin E may constitute a positive feedback loop, resulting in further increases in CDK activity, Rb phosphorylation, and "free" E2F. The products of E2F-regulated genes (including cyclins E and A) are thought to enable cells to enter S phase (13, 16, 17). It is not yet clear precisely how these signals regulate assembly and activation of the DNA replication machinery. Nevertheless, accumulation of sufficiently high levels of E2F is a critical determinant of entry into S phase. Indeed, forced expression of E2F alone is sufficient to stimulate quiescent cultured cells to replicate their DNA (18). Mitogenic G_1 signaling events are also subject to negative regulation. For example, CDK inhibitors (such as p21/CIP/WAF and p27) that are expressed in response to antiproliferative stimuli (*e.g.*, cytokines and genotoxic agents) can inhibit the kinase activity of CDKs, thereby eliciting proliferative arrest (19, 20).

In experiments described here, we have tested the effects of butyrate on cell cycle progression and on key signaling events that regulate passage through G_1. We show that butyrate induces expression of the p21 CDK inhibitor at the transcriptional level and that butyrate-induced cell cycle arrest results in large part from disruption of the Rb signaling axis. Surprisingly, however, we have found that p21 is dispensable for butyrate-induced growth arrest. Instead, inhibition of cyclin D1 expression provides a potential mechanism for butyrate-induced arrest in G_1.

Results

Butyrate-induced G_1 Arrest Is p53 Independent. The product of the *p53* tumor suppressor gene is stabilized and activated in response to a variety of growth-inhibitory stimuli, notably genotoxic agents such as UV light and ionizing radiation (20). When active, p53 can elicit growth arrest in the G_1 phase of the cell cycle or apoptosis (depending on cell type and nature of stimulus). Because butyrate is known to arrest many cell types in G_1 and is also reported to induce apoptosis in some cell lines, we considered the possibility

[3] The abbreviations used are: PDGF, platelet-derived growth factor; CDK, cyclin-dependent kinase; Rb, retinoblastoma protein; MEF, mouse embryo fibroblast; PDGFR, PDGF receptor; CAT, chloramphenicol acetyltransferase; HPV, human papilloma virus.

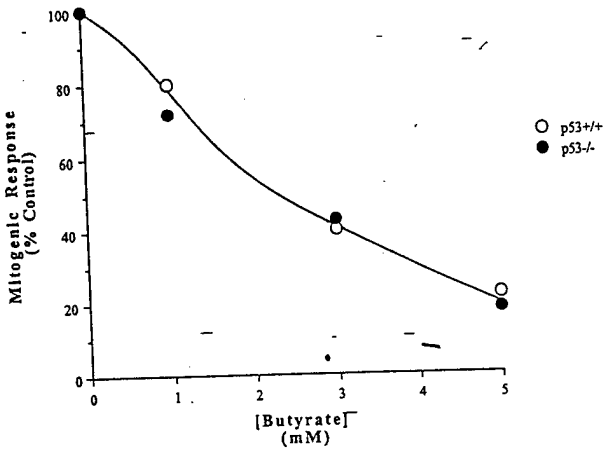

Fig. 1. Dose-response curves for inhibition of mitogenesis by butyrate in p53+/+ and p53−/− MEFs. Quiescent cultures of p53+/+ (○) or p53−/− (●) MEFs were stimulated with 10% serum for 24 h without or with varying doses of sodium butyrate and 1 μCi/ml of [^{3}H]thymidine. After 24 h of serum stimulation, the incorporation of tritiated thymidine into genomic DNA was determined by scintillation counting of solubilized nuclei, as described in "Materials and Methods." *Data points*, means of duplicate determinations, which differed by <5%. Error bars have been omitted for clarity.

that p53 may mediate these responses. Therefore, to test this hypothesis, we obtained primary cultured MEFs that had been derived from wild-type (p53+/+) and p53-deficient (p53−/−) transgenic animals (kindly provided by Dr. Tyler Jacks, Massachusetts Institute of Technology). To test whether p53 deficiency affected butyrate-induced G_1 arrest, we compared the susceptibility of p53+/+ and p53−/− cells to inhibition of G_1 progression by sodium butyrate.

We arrested the p53+/+ and −/− MEFs in G_0 by serum deprivation for 48 h. The resulting cultures of quiescent cells were stimulated to reenter the cell cycle with serum in the absence or presence of varying concentrations of butyrate. [^{3}H]Thymidine incorporation into genomic DNA was measured (as described in "Materials and Methods") to provide an index of entry into S phase. As shown in Fig. 1, butyrate prevented entry into S phase in a dose-dependent manner in both cell lines. The dose-response curves for butyrate-induced G_1 arrest in p53+/+ and p53−/− MEFs were indistinguishable. These data showed that lack of p53 did not preclude G_1 arrest in response to butyrate. Therefore, butyrate elicited G_1 arrest in a p53-independent manner.

Induction of p21 Transcripts during Butyrate-induced G_1 Arrest. Having eliminated a role for p53 in butyrate-induced G_1 arrest, we investigated alternative mechanisms whereby butyrate might inhibit progression through G_1. In recent years, the p21 CDK inhibitor, which negatively regulates cell cycle progression in G_1, has been shown to be expressed at high levels in response to a variety of antiproliferative stimuli (including some cytokines and DNA-damaging agents; reviewed in Refs. 19 and 20). We hypothesized that butyrate-induced G_1 arrest may be mediated by changes in p21 expression. p21-mediated G_1 arrest resulting from genotoxic agents is believed to result from a linear sequence of events involving activation of p53, transcriptional induction of the p21 gene by active p53, and inhibition of CDK activities by high level p21 expression (19, 20). Although our studies with p53-deficient MEFs suggested no role for p53 in butyrate-induced G_1 arrest, it remained possible that butyrate might elicit G_1 arrest in a p21-dependent (yet p53-independent) manner. Indeed, regions of the p21 promoter other than the p53-binding sites have been shown to be responsive to antiproliferative stimuli (such as those resulting from transforming growth factor β or induction of terminal differentiation; see Refs. 21 and 22).

Therefore, we tested the possible involvement of p21 in butyrate-induced cell cycle arrest. We performed RNA blotting experiments to analyze the expression of p21 mRNA under conditions of butyrate-induced cell cycle arrest. As shown in Fig. 2*a*, butyrate-treated 3T3 cells expressed high levels of p21 transcripts relative to control untreated fibroblasts. FACScan analysis of propidium iodide-stained nuclei from control and butyrate-treated cells indicated that 92% of the butyrate-treated cells were arrested in G_1, relative to 54% of control cells (Fig. 2*b*). The large fold induction of p21 mRNA levels during butyrate-induced G_1 arrest (Fig. 2) is comparable to the fold increase of p21 transcription that is elicited by other cytostatic agents.

Potentially, butyrate-induced p21 expression could have resulted from increased transcription of the *p21* gene or increased stability of the p21 transcript. While our studies were in progress, Nakano *et al.* (23) reported that butyrate-induced accumulation of p21 transcripts and activation of heterologous p21 promoter-luciferase constructs in a p53-deficient human colon adenocarcinoma cell line. This study demonstrated that p21 expression was transcriptionally induced by butyrate in a p53-independent manner. We performed similar experiments in p53-proficient and p53-compromised MEFs[4] and have obtained essentially similar results. In our experiments, heterologous p21 promoter-luciferase constructs with deletions or mutations in the p53-binding site also retained butyrate inducibility in p53-proficient as well as in p53-deficient cells. Because similar studies had already been published by another group (23), we chose not to duplicate those results here. Nevertheless, our unpublished experiments[4] and those of Nakano *et al.* (23) have shown that induction of p21 by butyrate can be accounted for by p53-independent transcriptional regulation.

p21 Is Not Required for Butyrate-induced G_1 Arrest. The experiments described above indicated a correlation between butyrate-induced p21 expression and G_1 arrest. To test the hypothesis that p21 mediated sodium butyrate-induced G_1 arrest, we studied the effects of butyrate on cell cycle progression in cultures of fibroblasts from p21-deficient (p21−/−) transgenic mice. We stimulated quiescent cultures of p21+/+ and p21−/− MEFs with serum in the presence of varying doses of butyrate. We measured the incorporation of [^{3}H]thymidine into genomic DNA to provide an index of G_1 progression and entry into S phase. Surprisingly, both the p21+/+ and p21−/− cells were susceptible to butyrate-induced cell cycle arrest in G_1 (Fig. 3). The dose-

[4] C. Vaziri and D. V. Faller, unpublished data.

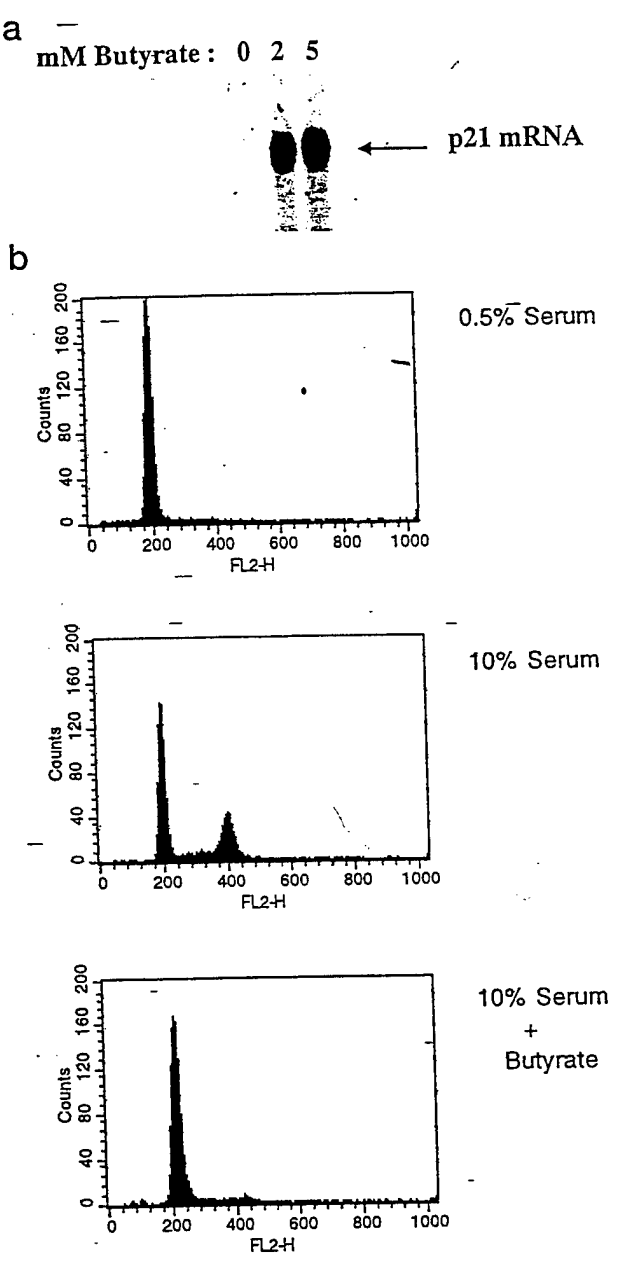

Fig. 2. Induction of p21 transcripts and G_1 arrest by butyrate in 3T3 fibroblasts. Exponentially growing cultures of 3T3 fibroblasts were treated with the indicated concentrations of butyrate for 24 h. *a*, RNA samples from control and butyrate-treated cells were analyzed for p21 expression by RNA blot analysis. In a parallel experiment, growing cells were placed in fresh serum-containing medium with or without 5 mM butyrate or in medium containing reduced-serum (0.5%). *b*, 24 hours later, the fibroblasts were analyzed for cell cycle distribution by FACScan analysis, as described in "Materials and Methods."

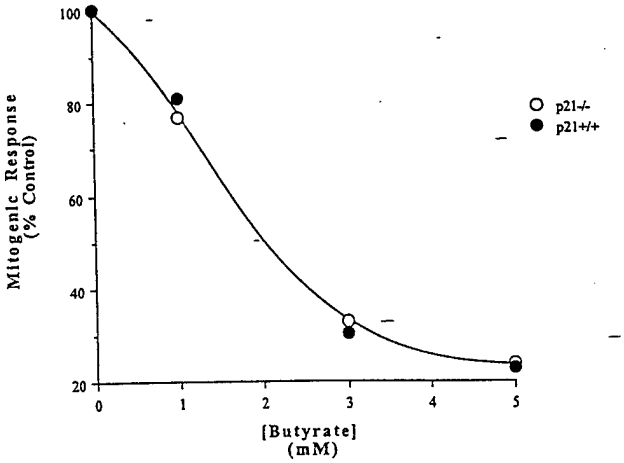

Fig. 3. Dose-response curves for inhibition of mitogenesis by butyrate in p21+/+ and p21−/− MEFs. Quiescent cultures of p21+/+ (●) or p21−/− (○) MEFs were stimulated with 10% serum for 24 h without or with varying concentrations of sodium butyrate and 1 μCi/ml [^{3}H]thymidine. Twenty-four h later, the incorporation of [^{3}H]thymidine into genomic DNA was measured as described in "Materials and Methods." *Data points*, means of duplicate determinations, which differed by <5%. Error bars have been omitted for clarity.

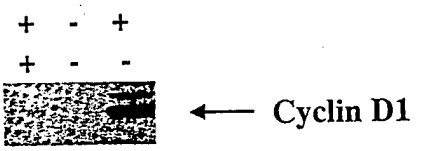

Fig. 4. Effects of butyrate on mitogen-induced cyclin D protein in 3T3 cells. Quiescent cultures of 3T3 cells were stimulated with 10% serum without or with 5 mM sodium butyrate for 12 h. At this time, cytosolic extracts were prepared from the cells. One hundred μg of each cytosolic extract was separated on a 10% polyacrylamide gel. After transfer to nitrocellulose, samples were probed with polyclonal antisera to cyclin D. Bound antibodies were visualized using alkaline phosphatase-conjugated secondary antisera.

response curves for butyrate-induced G_1 arrest in p21−/− and p21+/+ cells were indistinguishable (Fig. 3). These data showed that p21 was not required for butyrate-induced cell cycle arrest.

Butyrate Inhibition of Cyclin D1 Expression. The experiments described above indicated that p21-independent mechanism(s) must account for butyrate-induced inhibition of cell cycle progression. Transitions between different phases of the cell cycle are regulated by the activities of CDKs. CDK activities are, in turn, dependent upon the expression of appropriate cyclin proteins (reviewed in Refs. 13, 16, and 17). Thus, progression through G_1 and into S phase requires the sequential expression of cyclins D, E, and A (and concomitant activation of their CDK partners). Because butyrate arrested cell cycle progression during G_1, we asked whether mitogen-regulated expression of cyclins was perturbed by butyrate treatment. Therefore, we performed immunoblot analysis of cyclin expression in cell extracts from quiescent, serum-stimulated, and serum-plus butyrate-treated 3T3 fibroblasts. As expected, cyclin D protein levels were induced (relative to quiescent cells) at time points corresponding to mid-G_1 in serum-stimulated cells (Fig. 4). However, in the presence of butyrate, serum failed to induce cyclin D expression at these (or any other) time points. RNA blotting experiments showed that butyrate inhibited mitogen-induced accumulation of cyclin D1 transcripts in 3T3 cells, as well as in embryonic fibroblasts from p21+/+ and p21−/− mice (Fig. 5). To test the specificity of the effect of

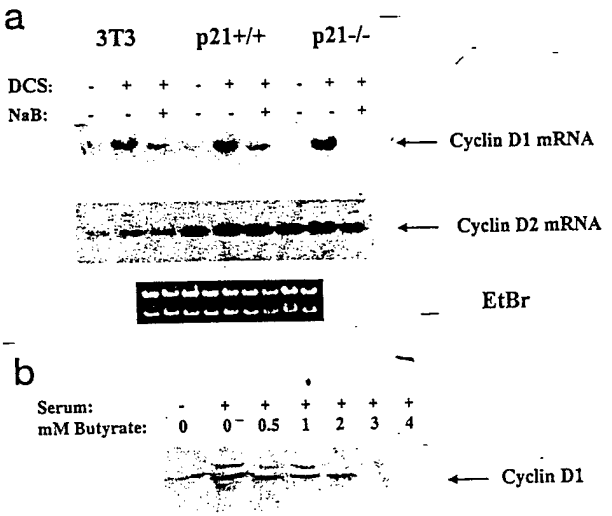

Fig. 5. Effect of butyrate on mitogen-induced cyclin D expression in p21+/+ and p21−/− MEFs. *a*, quiescent cultures of 3T3 fibroblasts, p21+/+ MEFs, and p21−/− MEFs were stimulated with 10% serum without or with 5 mM sodium butyrate. Eight h later, RNA was extracted from the cells. Twenty μg of total RNA from each sample were electrophoresed on a 1% agarose gel, transferred to nitrocellulose, and hybridized with a random-primed cyclin D1 cDNA probe. *Top*, autoradiogram of the washed blot; *middle*, autoradiogram of the same blot after reprobing with a random-primed cyclin D2 cDNA; *bottom*, a photograph of the ethidium bromide-stained 28S and 18S RNAs and provides a control for equivalent loading of samples. *b*, quiescent cultures of p21−/− MEFs were treated without or with 10% serum in the presence of varying concentrations of sodium butyrate for 8 h. At this time, cytosolic extracts were prepared from the cells. One hundred μg of each cytosolic extract were separated on a 10% polyacrylamide gel. After transfer to nitrocellulose, samples were probed with polyclonal antisera to cyclin D1 as described in "Materials and Methods."

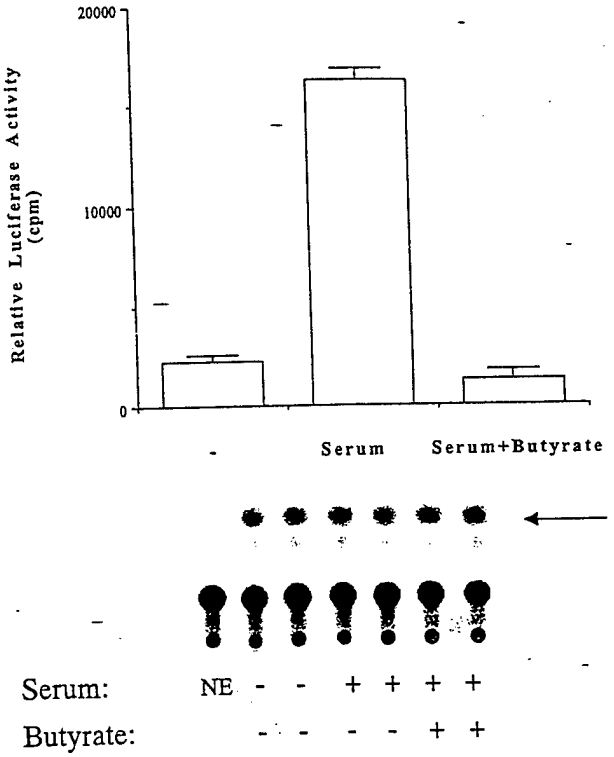

Fig. 6. Effect of butyrate on transiently transfected cyclin D1 promoter-driven reporter gene activity. 3T3 cells in 10-cm culture dishes were transfected overnight with 10 μg of −1745 D1-luciferase and 20 μg of −373 PDGF-βR-CAT using coprecipitation of plasmid DNAs with calcium phosphate. Transfected cells were placed in medium containing reduced (0.5%) serum to elicit growth arrest. The resulting quiescent cells were stimulated with 10% serum in the absence or presence of 5 mM sodium butyrate for 12 h. Cytosolic extracts were prepared as described in "Materials and Methods." A portion of each lysate was assayed for luciferase (*top*) and CAT (*bottom*) activity. *Bottom*, an autoradiogram of the developed TLC plate used to separate the products of the CAT reaction. *Arrow*, position of the diacetylated [^{14}C]chloramphenicol product.

butyrate on cyclin D1 expression, we also probed the RNA blot shown in Fig. 5 with a radiolabeled murine cyclin D2 cDNA. As shown in Fig. 5, butyrate treatment did not significantly affect cyclin D2 mRNA levels in any cell line tested. Surprisingly, 3T3 cells and embryonic fibroblasts from p21+/+ and p21−/− mice each expressed markedly different basal (and mitogen-stimulated) levels of cyclin D2 mRNA. The reason for the differential pattern of cyclin D2 expression between these cell types is not known. Nevertheless, these data showed that cyclin D1 mRNA expression was inhibited relatively specifically in a p21-independent manner. These results identified inhibition of cyclin D1 expression as a potential mechanism for p21-independent butyrate-induced growth arrest. Indeed, butyrate inhibited cyclin D1 expression and G_1 progression with a similar dose dependencies (please compare butyrate concentrations used in Figs. 3 and 5*b* for inhibition of mitogenesis and cyclin D expression, respectively, in p21−/− cells).

Mechanism of Inhibition of Cyclin D1 Expression by Butyrate. The butyrate-induced changes in cyclin D1 expression could potentially have resulted from decreased stability of cyclin D1 mRNA or from reduced transcription of the *cyclin D1* gene. To distinguish between these possibilities, we performed transient transfection experiments using a heterologous reporter gene construct containing the promoter region of the *cyclin D1* gene linked to a luciferase reporter cDNA (designated −1745 D1-LUC). Cultures of 3T3 cells were cotransfected with the cyclin D1 promoter-luciferase construct and a PDGFR promoter-CAT reporter construct (as an internal control). The transfected cultures of fibroblasts were rendered quiescent by serum starvation for 24 h. The resulting cells were then incubated for an additional 12 h with 10% serum in the absence or presence of 5 mM butyrate (or with no serum as a control). At this time, cytosolic extracts were harvested from the cells as described in "Materials and Methods." Each extract was assayed for both luciferase and CAT activity (to provide indications of cyclin D1 and PDGFR promoter-driven reporter gene expression, respectively). As expected, serum stimulation induced expression of the cyclin D1 promoter-driven luciferase reporter gene relative to control quiescent cultures. However, in the presence of butyrate, mitogen-stimulated luciferase activity was fully attenuated (Fig. 6). Therefore, butyrate prevented serum-dependent activation of the cyclin D1 promoter. The effect of butyrate on the cyclin D1 promoter was relatively specific because PDGFR promoter-dependent transcription of a CAT cDNA in the same cultures of 3T3 cells was unaf-

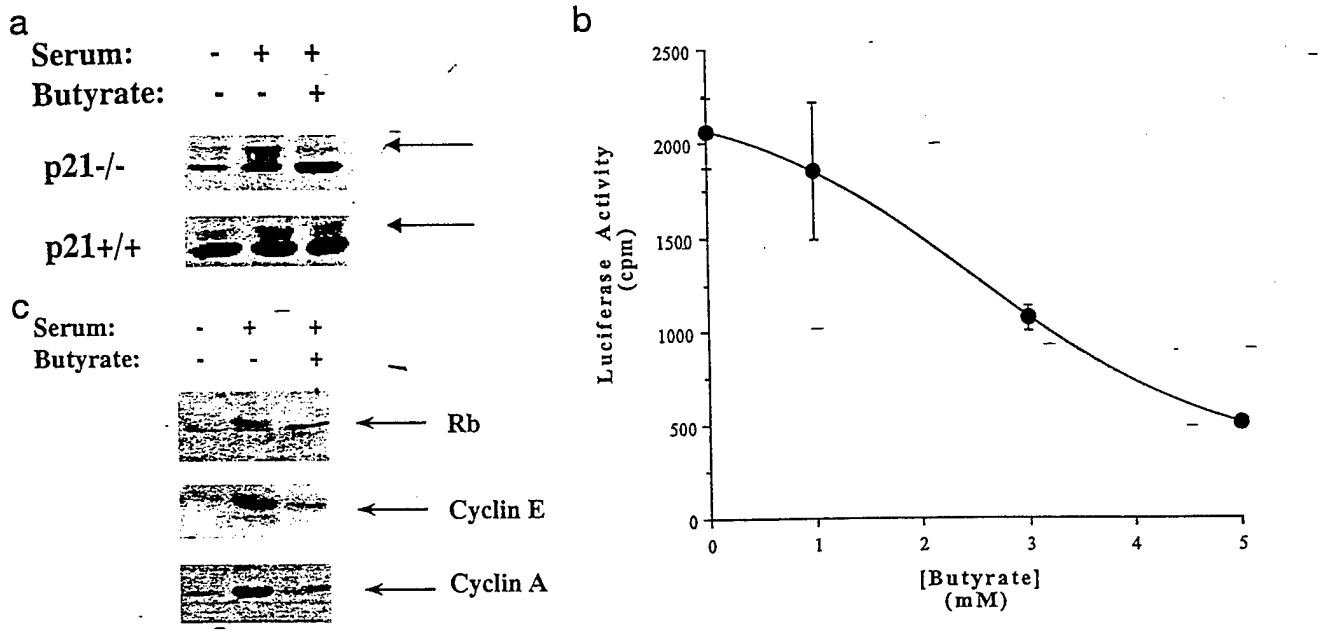

Fig. 7. Effects of butyrate on mitogen-dependent Rb phosphorylation and expression of cyclins E and A in 3T3 fibroblasts. *a*, quiescent cultures of p21+/+ and p21−/− cells were stimulated with 10% serum without or with 5 mM sodium butyrate for 13 h. At this time, cytosolic extracts were prepared from the cells. One hundred μg of each cytosolic extract were separated on a 6% polyacrylamide gel. After transfer to nitrocellulose, samples were probed with polyclonal antisera to Rb. Bound antibodies were visualized using an ECL kit (Amersham). *Arrows*, positions of the slowly migrating hyperphosphorylated Rb bands. *b*, construct containing the promoter region of the murine cyclin E gene upstream of a firefly luciferase cDNA was stably transfected into 3T3 cells as described in "Materials and Methods." Quiescent cultures of stably transfected cells were stimulated without or with 10% serum and varying doses of sodium butyrate for 13 h. Detergent lysates from the cells were normalized for protein content and assayed for luciferase activity, as described in "Materials and Methods." In the experiment shown, luciferase activity in unstimulated cells (which received neither serum nor butyrate) was 238 ± 146 cpm. *c*, quiescent cultures of 3T3 cells were stimulated with 10% serum without or with 5 mM sodium butyrate for 13 h. At this time, cytosolic extracts were prepared from the cells. One hundred μg of each cytosolic extract were separated on a 6% polyacrylamide gel. After transfer to nitrocellulose, samples were probed with polyclonal antisera to Rb (*top*), cyclin E (*middle*), or cyclin A (*bottom*). Bound antibodies were visualized using alkaline phosphatase-conjugated secondary antisera.

fected by butyrate (Fig. 6). These data demonstrated that relatively specific transcriptional mechanisms could account for inhibition of cyclin D1 expression in response to butyrate.

Butyrate Perturbs G_1 Signaling Events Distal to Cyclin D Expression. When activated, cyclin D-dependent kinases (CDKs 4 and 6) phosphorylate multiple sites upon the Rb tumor suppressor protein (13, 16, 17). Phosphorylation of Rb by CDKs relieves an inhibitory constraint that is imposed by hypophosphorylated Rb upon the E2F transcription factor family of proteins. Thus, phosphorylation of Rb by CDKs enables the transcriptional activation of E2F-regulated genes (including those encoding cyclins E and A, dihydrofolate reductase, and many others), the products of which are thought to mediate entry into S phase. As described above, butyrate treatment prevented mitogen-induced expression of cyclin D1. Therefore, we tested whether inhibition of cyclin D by butyrate was sufficient to perturb more distal mitogenic events, namely, Rb phosphorylation and activation of E2F-dependent promoters.

Hyperphosphorylated Rb protein migrates with a characteristic retarded electrophoretic mobility (relative to hypophosphorylated Rb) on SDS-polyacrylamide gels. We tested whether butyrate treatment affected the phosphorylation of Rb, a process known to be carried out by active cyclin D-CDK complexes during mid- to late G_1. We performed immunoblot analysis of cytosolic lysates from quiescent, serum-stimulated, and serum-plus butyrate-treated cells using an anti-Rb antibody. As expected, serum stimulation elicited a band shift characteristic of hyperphosphorylated Rb in both p21+/+ and p21−/− MEFs (Fig. 7*a*). However, this mobility shift did not occur in Rb that was present in lysates from butyrate-treated cells (Fig. 7*a*). Therefore, butyrate prevented mitogen-dependent phosphorylation of Rb in a p21-independent manner.

As already noted, hypophosphorylated Rb negatively regulates E2F activation and entry into S phase. Entry into S phase is mediated by transcriptional induction of E2F-regulated genes, including *cyclin E*. We tested whether butyrate inhibition of Rb phosphorylation was sufficient to perturb downstream E2F-dependent events. We generated a 3T3 cell line stably expressing a plasmid containing 895 bp of the 5′ region of the murine *cyclin E* gene linked to a luciferase reporter cDNA. Mitogen-regulated transcription of the luciferase reporter gene from this construct is entirely dependent upon E2F sites within this region of the promoter (24). As expected, serum induced an increase (~8-fold in the experiment shown) in the expression of cyclin E promoter-driven luciferase activity in the stably transfected cells (Fig. 7*b*). Serum-induced luciferase activity was inhibited by sodium butyrate in a dose-dependent manner (Fig. 7*b*). The dose-response curves for inhibition of cyclin E promoter activity by

butyrate were similar to the values we obtained for inhibition of mitogenesis and cyclin D expression.

To further test our hypothesis that Rb-dependent events are perturbed by butyrate, we performed immunoblot analysis of cyclin E and cyclin A proteins (the mitogen-induced expression of which is mediated by E2F sites within the promoter regions of the genes encoding these proteins) in quiescent, mitogen-stimulated, and mitogen- and butyrate-treated cells. As shown in Fig. 7*c*, the serum-dependent expression of both cyclins A and E was prevented by butyrate, concomitantly with inhibition of Rb phosphorylation. Overall, the data described above showed a good correlation between perturbation of the Rb signaling pathway and butyrate-induced G_1 arrest.

HPV-E7-expressing Cells Display Increased Resistance to Butyrate-induced G_1 Arrest. Our data suggested that butyrate-induced disruption of the Rb signaling pathway may cause G_1 arrest. To test this hypothesis we adopted a "loss of function approach" and engineered 3T3-derived cell lines with defects in Rb function. When expressed, certain viral oncoproteins such as the HPV E7 protein, bind to and sequester Rb and the Rb-related p107 and p130 pocket proteins. The binding of Rb by viral oncoproteins abrogates the requirement for Rb phosphorylation which ordinarily regulates E2F transcriptional activity (25, 26). Deregulated E2F activity in HPV E7-expressing cells is thought to contribute to defective checkpoint controls and aberrant proliferation. We have used retroviral vectors to generate 3T3 cells expressing stably integrated *HPV E7* genes. As expected, the resulting E7-expressing cells displayed high levels of E2F activity, grew to high density, and showed a high degree of serum-independent proliferation relative to control cell lines that were infected with an "empty" retroviral vector (data not shown). Therefore, E7 expression resulted in loss of normal Rb-mediated checkpoints in these cells.

We compared the butyrate sensitivity of mitogen-stimulated G_1 progression in control cells expressing vector alone (designated "SXSN"), cells expressing the HPV E6 gene (which when expressed elicits ubiquitination and proteolysis of p53; see Ref. 27), and cells expressing stably integrated HPV E7, alone or in combination with the E6 gene (designated "SE7" and "SE6E7" respectively). As expected, abrogation of p53 function by E6 expression had no effect on sensitivity to butyrate-induced G_1 arrest. However, cell lines expressing HPV E7 (alone or in combination with E6) displayed markedly increased resistance to butyrate-induced growth arrest. As shown in Fig. 8 a dose of 3 mM butyrate, which elicited 80% inhibition of S-phase entry in control (or HPV E6-expressing) cells, only inhibited entry into S phase by ~38% in HPV E7-expressing fibroblasts. These data showed that functional inactivation of Rb (and other pocket proteins) but not of p53 resulted in decreased sensitivity to the cytostatic actions of butyrate. These data support our hypothesis that butyrate-induced G_1 arrest in normal cells results, in large part, from a p53-p21-independent perturbation of the Rb signaling axis.

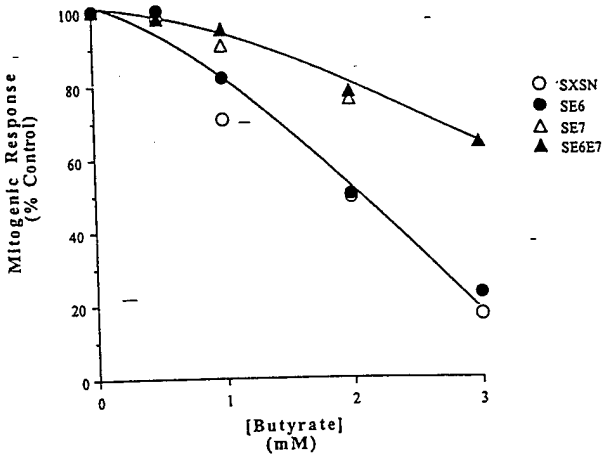

Fig. 8. Effect of HPV oncoprotein expression on sensitivity to butyrate-induced G_1 arrest in 3T3 cells. Retroviral vectors were used to express HPV E6, E7, and E6 and E7 cDNAs in 3T3 cells. As a control, 3T3 cells were infected with an empty retroviral vector lacking an ectopic gene. The resulting cells were designated SXSN (○), SE6 (●), SE7 (△), and SE6E7 (▲) and expressed empty vector, E6 cDNA, E7 cDNA, and E6 plus E7 cDNAs, respectively. Cultures of serum-starved cells containing empty vector or viral oncoproteins were stimulated with 10% serum for 24 h, without or with varying concentrations of sodium butyrate and 1 μCi/ml of [^{3}H]thymidine. After 24 h, the incorporation of tritiated thymidine into genomic DNA was determined by scintillation counting of solubilized nuclei as described in "Materials and Methods." These values are expressed as percentage maximal serum-stimulated mitogenic response in the absence of butyrate. *Data points*, means of duplicate determinations, which differed by <5%. Error bars have been omitted for clarity.

Discussion

Although butyrate is known to inhibit cell cycle progression, the molecular basis of butyrate-induced G_1 arrest has not been elucidated. We and others have hypothesized that inhibition of cell cycle progression in response to butyrate results from modification of mitogenic signal transduction event(s) during G_1. In this report, we have tested the effects of butyrate on mitogen-induced G_1 signaling events. Because p53 mediates growth inhibition in response to a variety of stimuli, we initially investigated a possible role for p53 in butyrate-induced G_1 arrest. Our results demonstrate that p53-deficient cells (p53−/− MEFs from transgenic animals and fibroblasts expressing the HPV E6 oncoprotein in which p53 levels and activity are markedly reduced) remain susceptible to butyrate-induced growth arrest. These data suggest that p53 does not mediate butyrate-induced G_1 arrest. Because ~50% of human tumors have defects in p53 signaling, our finding that p53-compromised cells are responsive to butyrate-induced growth inhibition further emphasizes the potential value of butyrate and related compounds for cancer therapy.

Interestingly, we have shown that expression of the *p21* CDK inhibitor gene (which is a mediator of p53-dependent G_1 arrest) is induced by butyrate in a p53-independent manner in untransformed 3T3 cells (as well as in transformed 3T3 lines).[5] These data corroborate recent results from other

[5] C. Vaziri, L. Stice, and D. V. Faller, unpublished observations.

workers who have also demonstrated p53-independent transcriptional induction of p21 in colon cancer cells (23). Because p21 inhibits the activities of CDKs which regulate cell cycle progression, these data suggested a potential mechanism for butyrate-induced G_1 arrest. Therefore we tested the hypothesis that p21 may mediate growth arrest in response to butyrate. We examined the susceptibility of p21-deficient cells to butyrate-induced G_1 arrest. Surprisingly, p21−/− cells (from transgenic animals with a p21-null genetic background) were as sensitive as p21-proficient (p21+/+) cells to butyrate-induced growth arrest. These unexpected results suggested the existence of p21-independent pathways of butyrate-induced growth arrest.

To identify putative p21-independent butyrate-induced lesions in G_1 mitogenic signaling events we analyzed the expression of the G_1 cyclins in cultures of synchronized fibroblasts. Cyclins are known to regulate transitions between different phases of the cell cycle. Cyclin D, which is transcriptionally induced during mid-G_1, is the first cyclin to be expressed following mitogen-stimulated entry into the cell cycle (13). Our experiments have shown that butyrate inhibited mitogen-dependent expression of cyclin D1 mRNA and protein. In addition, our transient transfection experiments using a heterologous cyclin D1 promoter-luciferase construct showed that transcriptional mechanisms could account for the effect of butyrate on cyclin D1 expression. The dose dependency for inhibition of cyclin D expression by butyrate paralleled that of G_1 arrest in p21-deficient (and p21-proficient) cells. Therefore, inhibition of cyclin D expression provides a mechanism for p21-independent butyrate-induced G_1 arrest. Interestingly, expression of cyclin D2 mRNA was not significantly affected by butyrate, suggesting that this D-type cyclin cannot compensate for cyclin D1 deficiency resulting from butyrate. It has been suggested previously that the butyrate cell cycle block is related to termination of expression of a labile protein (7). Potentially, cyclin D1 may represent this (putative) labile protein.

Consistent with a putative role for cyclin D1 suppression in butyrate-induced G_1 arrest, we have shown that mitogenic events temporally distal to cyclin D expression (CDK activation and Rb phosphorylation, cyclin E expression, and cyclin A expression) are inhibited by butyrate. Furthermore, abrogation of a requirement for cyclin D-dependent kinase activity and Rb phosphorylation by expression of the HPV E7 oncoprotein conferred resistance to the growth-inhibitory actions of butyrate. Overall, these data suggest that butyrate elicits G_1 arrest by perturbing the mitogen-dependent induction of cyclin D1 (and, consequently, also Rb-mediated signaling events that normally occur distal to cyclin D1 expression). Interestingly, Wintersberger *et al.* (4) noted that SV40-transformed cells displayed reduced sensitivity to butyrate-induced G_1 arrest. Like the HPV E7 oncoprotein, SV40 large T antigen contributes to cellular transformation by binding and inactivating Rb (and other pocket proteins). Therefore, abrogation of a requirement for cyclin D-dependent kinase activity in SV40-transformed cells is likely to have conferred the increased resistance to butyrate that was observed in the experiments of Wintersberger and colleagues (4).

Although HPV E7 expression in our study [and SV40 transformation in the report by Wintersberger *et al.* (4)] did confer significant resistance to butyrate-induced G_1 arrest, high concentrations of butyrate did eventually inhibit entry into S phase in these experiments. Cyclin E- and A-dependent kinases are normally activated subsequent to cyclin D-CDK and are essential for progression into S phase, even in the absence of functional Rb. It is possible that induction of p21 expression by butyrate, and p21-mediated inhibition of cyclin E- and cyclin A-dependent kinases elicited G_1 arrest in the viral oncoprotein-expressing cells. Therefore, our data suggest the existence of at least two butyrate-induced lesions in mitogenic G_1 signaling events: one at the level of cyclin D1 expression, another resulting from p21 induction.

At least two other groups have noted effects of butyrate on the expression of cyclin D1. Siavoshian *et al.* (14) demonstrated an increase in cyclin D expression in butyrate-treated HT29 (human colon cancer) and HBL-100 (mammary epithelial) cells (14). In contrast, Lallemand *et al.* (15) showed that butyrate inhibited cyclin D expression in benzo(*a*)pyrene-transformed BP-A31 fibroblasts. Our data are similar to those reported by the latter group. The murine fibroblast cell lines that we have used in our experiments are likely to be more closely related to the BP-A31 cell line (a fibroblast line originally derived from Balb/c-3T3 fibroblasts) used by Lallemand *et al.* (15). It is possible that mesenchymal cells [such as the ones used in our study and the experiments of Lallemand and colleagues (15)] respond differently from epithelial cells [*e.g.*, those used by Siavoshian and coworkers (14)] with respect to cyclin D expression. Interestingly, butyrate was found to stimulate p21 expression in HT29 cells. Therefore, it is likely that induction of p21 (but not changes in cyclin D1 expression) resulting from butyrate treatment contribute to G_1 arrest in this cell type.

Experiments are currently underway in our laboratory to understand the mechanisms whereby butyrate perturbs cyclin D1 expression in normal untransformed mesenchymal lines. Our data and the results of Lallemand *et al.* (15) have shown that butyrate inhibits expression of a luciferase reporter gene driven by the cyclin D1 promoter. Transcription of the cyclin D1 gene is thought to require the prior transduction of mitogen-regulated signaling events (including second messenger signals, protein kinase cascades, and transcription of immediate-early response genes). The specific signaling cascades and transcription factors that mediate mitogen-dependent expression of the cyclin D1 gene have not yet been identified. However, the promoter region of the cyclin D1 gene is known to be responsive to ectopically expressed v-*ras* and c-*jun* proto-oncogenes (28). Both c-ras and c-jun proteins are considered to play important roles in mitogen-stimulated cell cycle progression and may have physiologically relevant roles in regulation of cyclin D1 expression. Therefore, signaling cascades involving ras and c-jun represent potential targets for the growth-inhibitory actions of sodium butyrate. Potentially, butyrate may perturb the ordered regulation of these mitogen-induced second messenger and transcriptional events. Alternatively, butyrate might exert a direct effect on transcriptional regulation of the

cyclin D1 gene, for example, direct modification of transcription factor–DNA interactions at the cyclin D1 promoter.

Many studies have shown that butyrate and related compounds affect chromatin structure and gene expression (29–31). Butyrate is known to inhibit the activity of histone deacetylases (2, 29). Recent studies suggest that histone acetylation is an important transcriptional regulatory mechanism (32). Histone acetylation can alter nucleosomal positioning resulting in derepression of gene transcription (32–34). It is possible, therefore, that many of the effects of butyrate on gene expression result from changes in the acetylation state of histones. Cell cycle progression requires regulation and integration of numerous transcriptional events. It is possible that deregulation of these events by butyrate (due to changes in histone acetylation) perturbs progression through G_1.

Yoshida and Beppu (35) have reported that trichostatin A, a potent and selective inhibitor of histone deacetylase activity, can elicit arrest in G_1 and in G_2 in rat 3Y1 cells (35). We have obtained similar results in experiments with 3T3 cells.[6] It is possible, therefore, that butyrate-induced G_1 arrest results, in large part, from hyperacetylation of histones. Our laboratory has recently developed a series of butyrate analogues and derivatives for treatment of β-thalassemia and other disorders of globin expression (36–38). Not all of these compounds affect histone deacetylase activity. We plan to test whether these compounds affect cell cycle progression and mitogen-regulated signaling events (*e.g.*, cyclin D1 expression). These experiments may enable us to establish correlations (or dissociate between) inhibition of histone deacetylase and cell cycle-regulated events (*e.g.*, p21, cyclin D1 expression, and G_1 progression).

In conclusion, we have shown that butyrate elicits G_1 arrest, in large part, by perturbing the Rb signaling axis. At least two distinct mechanisms contribute to butyrate-induced G_1 arrest: (*a*) inhibition of cyclin D1 expression and (*b*) p53-independent induction of p21. Further studies are in progress to identify the specific molecular lesions that mediate changes in cyclin D1 and p21 expression.

Materials and Methods

Cells and Culture. p21−/− and p53−/− MEFs and appropriate wild-type control cell lines were provided by Drs. P. Leder (Harvard Medical School) and T. Jacks (Massachusetts Institute of Technology), respectively. Murine 3T3 cell lines (Balb 3T3, NIH 3T3, and Swiss 3T3 cells) were obtained from the American Type Culture Collection. Identical results were obtained with all three 3T3 cell lines. All cells were cultured in DMEM containing 10% heat-inactivated bovine serum supplemented with glutamine and penicillin-streptomycin. HPV E6- and E7-expressing 3T3 cells were generated by retroviral infection as described previously (39). Stably infected cells were selected in medium containing 0.5 mg/ml G418. To avoid artifacts due to clonal selection of aberrant cells, experiments were performed with pools of G418-resistant cells. To generate cell lines stably expressing the cyclin E promoter-luciferase construct Swiss 3T3 cells were cotransfected with 30 μg of pCyc E −795/+100 (24) and 2 μg of the pCIneo construct (Promega) to enable selection of transfected cells. Stably transfected cells were selected in medium containing 0.5 mg/ml G418. Experiments were performed using pooled colonies of G418-resistant cells.

Transient Transfections and Reporter Gene Analysis. 3T3 cells in 10-cm culture dishes were transfected overnight with 10 μg of −1745 D1-luciferase and 20 μg of −373 PDGF βR-CAT using coprecipitation of plasmid DNAs with calcium phosphate. Transfected cells were placed in medium containing reduced (0.5%) serum to elicit growth arrest. The resulting quiescent cells were stimulated with 10% serum in the absence or presence of 5 mM sodium butyrate for 12 h. To assay reporter gene activity, the monolayers of fibroblasts were washed twice with 10 ml of PBS. The washed cells were then scraped into 1× reporter lysis buffer (Promega). To obtain cytosolic extracts, the suspensions of cells were subject to two freeze-thaw cycles and centrifuged (10,000 × *g*; 5 min) to remove nuclei and cellular debris. After normalizing for protein content, aliquots of the clarified cytosolic supernatants were assayed for both luciferase and CAT activities according to standard protocols.

Mitogenic Assays and FACScan Analysis. To elicit growth arrest, near-confluent cultures of cells were placed in medium containing 0.5% serum for 48 h. Serum-starved cultures were stimulated to enter the cell cycle by addition of fresh serum (to a final concentration of 10%) to the starvation medium. In some experiments, 1 μCi/ml [^{3}H-methyl]thymidine was added to the cultures at the time of serum stimulation. To determine relative rates of DNA synthesis, the incorporation of [^{3}H]thymidine into genomic DNA was determined by NaOH/SDS solubilization of trichloroacetic acid-fixed cells as described previously (39). For FACScan analysis, monolayers of cells were washed in PBS, detached from the culture dish with trypsin-EDTA, fixed in 35% ethanol, stained with propidium iodide, and then analyzed on a Becton Dickinson flow cytometer as described previously (39).

RNA Blot Analysis. RNA was extracted from cells according to the single step method of Chomczynski and Sacchi (40). Twenty-μg samples of total RNA were electrophoresed on formaldehyde/agarose gels as described previously (39). The separated RNAs were transferred to nitrocellulose filters and probed with random-primed ^{32}P-labeled cDNAs. Hybridization and high-stringency wash conditions were performed as described previously (39).

Immunoblotting. Cytosolic extracts were prepared by detergent lysis as described previously (39). Electrophoretic separation of proteins, transfer to nitrocellulose filters, and probing and detection of antigens were performed as described previously (39). The antibodies used in this study were purchased from Santa Cruz Biotechnology (antimurine cyclins D1, E, and A rabbit polyclonal antibodies) and PharMingen (antihuman Rb monoclonal antibody).

Reproducibility and Statistical Analysis. All data shown are representative of results from experiments which were performed at least three times. Similar results were obtained on each occasion. All data points shown are means of duplicates, which differed by <5%. On some graphs containing multiple data points, error bars have been omitted for clarity.

Acknowledgments

We thank Drs. Philip Leder and Tyler Jacks for p21−/− and p53−/− MEFs, respectively. Dr. Charles Sherr kindly provided the murine cyclin D1- and D2 cDNAs. HPV retroviral vectors and cDNAs were generous gifts from Drs. Denise Galloway and Karl Munger. Dr. Peter Jansen-Durr kindly provided the Cyclin E-Luciferase construct. The cyclin D1-Luciferase construct was generously provided by Dr. Richard G. Pestell.

References

1. Cummings, J. H., Pomare, E. W., Branch, W. J., Naylor, C. P. E., and MacFarlane, G. T. Short chain fatty acids in human large intestine, portal, hepatic, and venous blood. Gut, *28:* 1221–1227, 1987.

2. D'Anna, J. A., Tobey, R. A., and Gurley, L. R. Concentration-dependent effects of sodium butyrate in Chinese hamster cells: cell cycle progression, inner histone acetylation, histone H1 dephosphorylation, and induction of an H1-like protein. Biochemistry, *19:* 2656–2971, 1980.

3. Daniell, E. Cells inhibited by butyrate support adenovirus replication. Virology, *107:* 514–519, 1980.

4. Wintersberger, E., Mudrak, I., and Wintersberger, U. Butyrate inhibits mouse fibroblasts at a control point in the G_1 phase. J. Cell. Biochem., *21:* 239–247, 1983.

[6] L. Stice and D. V. Faller, unpublished data.

5. Staiano-Coico, L., Steinberg, M., and Higgins, P. J. Epidermal cell shape regulation and subpopulation kinetics during butyrate-induced terminal maturation of normal and SV40-transformed keratinocytes: epithelial models of differentiation therapy. Int. J. Cancer, *46:* 733–738, 1990.

6. Balk, S., Gunther, H., and Morisi, A. Butyrate reversibly arrests the proliferation of normal and Rous sarcoma virus-infected chicken heart mesenchymal cells. Life Sci., 803–808, 1984.

7. Campisi, J., Medrano, E. E., Morreo, G., and Pardee, A. Restriction point control of cell growth by a labile protein: evidence for increased stability in transformed cells. Proc. Natl. Acad. Sci. USA, *79:* 436–440, 1982.

8. Medrano, E. E., and Pardee, A. B. Prevalent deficiency in tumor cells of cycloheximide-induced cycle arrest. Proc. Natl. Acad. Sci. USA, *77:* 4123–4126, 1980.

9. Boffa, L. C., Lupto, J. R., Mariani, M. R., Ceppi, M., Newmark, H. L., Scamati, A., and Lipkin, M. Modulation of colonic epithelial cell proliferation, histone acetylation, and luminal short chain fatty acids by variation of dietary fiber (wheat bran) in rats. Cancer Res., *52:* 5906–5912, 1992.

10. Hague, A., Manning, A. M., Hanlon, K. A., Huschtscha, L. I., Hart, D., and Paraskeva, C. Sodium butyrate induces apoptosis in human colonic tumour cell lines in a p53-independent pathway: implications for the possible role of dietary fibre in the prevention of large bowel cancer. Int J. Cancer, *55:* 498–505, 1993.

11. Pardee, A. B. G_1 events and regulation of cell proliferation. Science (Washington DC), *240:* 603–608, 1989.

12. Cantley, L. C., Auger, K. R., Carpenter, C., Duckworth, B., Graziani, A., Kapeller, R., and Soltoff, S. Oncogenes and signal transduction. Cell, *64:* 281–302, 1991.

13. Sherr, C. J. Mammalian G_1 cyclins. Cell, *73:* 1059–1065, 1993.

14. Siavoshian, S., Blottiere, H. M., Cherbut, C., and Galmiche, J. P. Butyrate stimulates cyclin D and p21 and inhibits cyclin-dependent kinase 2 expression in HT-29 colonic epithelial cells. Biochem. Biophys. Res. Commun., *232:* 169–172, 1997.

15. Lallemand, F., Courilleau, D., Sabbah, M., Redeuilh, G., and Mester, J. Direct inhibition of the expression of cyclin D1 gene by sodium butyrate. Biochem. Biophys. Res. Commun., *229:* 163–169, 1996.

16. Weinberg, R. A. The retinoblastoma protein and cell cycle control. Cell, *81:* 323–330, 1995.

17. Herwig, S., and Strauss, M. The Rb protein: a master regulator of cell cycle, differentiation and apoptosis. Eur. J. Biochem., *246:* 581–601, 1997.

18. Johnson, D. G., Schwarz, J. K., Cress, W. D. and Nevins, J. R. Expression of transcription factor E2F1 induces quiescent cells to enter S-phase. Nature (Lond.), *365:* 349–352, 1993.

19. Sherr, C. J., and Roberts, J. M. Inhibitors of mammalian G_1 cyclin-dependent kinases. Genes Dev., *9:* 1149–1163, 1995.

20. Ko, L. J., and Prives, C. p53: puzzle and paradigm. Genes Dev., *10:* 1054–1073, 1996.

21. Steinman, R. A., Hoffman, B., Iro, A., Guillouf, C., Lieberman, D. A., and el-Houseini, M. E. Induction of p21 (WAF-1/CIP1) during differentiation. Oncogene, *9:* 3389–3396, 1996.

22. Datto, M. B., Yu, Y., and Wang, X. F. Functional analysis of the transforming growth factor β responsive elements in the WAF1/Cip1/p21 promoter. J. Biol. Chem., *270:* 28623–28628, 1995.

23. Nakano, K., Mizuno, T., Sowa, Y., Orita, T., Yoshino, T., Okuyama, Y., Fujita, T., Ohtani-Fujita, N., Matsukawa, Y., Tokino, T., Yamagishi, H., Oka, T., Nomura, H., and Sakai, T. Butyrate activates the WAF-1/CIP1 gene promoter through sp1 sites in a p53-negative colon cancer cell line. J. Biol. Chem., *272:* 22199–22206, 1997.

24. Botz, J., Zerfass-Thome, K., Spitkovsky, D., Delius, H., Vogt, B., Eilers, M., Hatzigeorgiou, A., and Jansen-Durr, P. Cell cycle regulation of the murine cyclin E gene depends on an E2F binding site in the promoter. Mol. Cell. Biol., *16:* 3401–3409, 1996.

25. Munger, K., Werness, B. A., Dyson, N., Phelps, W. C., Harlow, E., and Howley, P. M. Complex formation of human papillomavirus E7 proteins with the retinoblastoma tumor suppressor gene product. EMBO J., *8:* 4099–4105, 1989.

26. Nevins, J. R. E2F: a link between the Rb tumor suppressor protein and viral oncoproteins. Science (Washington DC), *258:* 424–429, 1992.

27. Werness, B. A., Levine, A. J., and Howley, P. M. Association of human papillomavirus types 16 and 18 E6 proteins with p53. Science (Washington DC), *248:* 76–79, 1990.

28. Albanese, C., Johnson, J., Watanabe, G., Eklund, N., Vu, D., Arnold, A., and Pestell, R. G. Transforming p21 ras mutants and c-Ets-2 activate the cyclin D1 promoter through distinguishable regions. J. Biol. Chem., *270:* 23589–23597, 1995.

29. Gorman, C. M., Howard, B. H., and Reeves, R. Expression of recombinant plasmids in mammalian cells is enhanced by sodium butyrate. Nucleic Acids Res., *11:* 7631–7648, 1983.

30. Klehr, D., Schlake, T., Maass, K., and Bode, J. Scaffold-attached regions (SAR elements) mediate transcriptional effects due to butyrate. Biochemistry, *31:* 3222–3229, 1992.

31. Candido, E. P. M., Reeves, R., and Davie, J. R. Sodium butyrate inhibits histone deacetylation in cultured cells. Cell, *14:* 105–113, 1978.

32. Turner, B. M. Histone acetylation and control of gene expression. J. Cell Sci., *99:* 13–20, 1991.

33. Wolffe, A. P., and Pruss, D. Targeting chromatin disruption: transcription regulators that acetylate histones. Cell, *84:* 817–819, 1996.

34. Grunstein, M. Histone acetylation in chromatin structure and transcription. Nature (Lond.), *389:* 349–352, 1997.

35. Yoshida, M., and Beppu, T. Reversible arrest of proliferation of rat 3Y1 fibroblasts in both the G_1 and G_2 phases by trichostatin A. Exp. Cell Res., *177:* 122–131, 1988.

36. Faller, D. V., and Perrine, S. P. Butyrate in the treatment of sickle cell disease and β-thalassemia. Curr. Opin. Hematol., *2:* 109–117, 1995.

37. Boosalis, M. S., Ikuta, T., Pace, B. S., daFonseca, S., White, G. L., Faller, D. V., and Perrine, S. P. Abrogation of Il-3 requirements and stimulation of hematopoetic cell proliferation *in vitro* and *in vivo* by carboxylic acids. Blood Cells Mol. Dis., *23:* 434–442, 1997.

38. Torkelson, S., White, B., Faller, D. V., Phipps, K., Pantazis, C., and Perrine, S. P. Erythroid progenitor proliferation is stimulated by phenoxyacetic and phenylalkyl acids. Blood Cells Mol. Dis., *22:* 150–158, 1996.

39. Vaziri, C., and Faller, D. V. A benzo[a]pyrene-induced cell cycle checkpoint resulting in p53-independent G_1 arrest in 3T3 fibroblasts. J. Biol. Chem., *272:* 2762–2769, 1997.

40. Chomczynski, P., and Sacchi, N. Single step method of RNA isolation by acid guanidinium thiocyanate-phenol-chloroform extraction. Anal. Biochem., *162:* 156–159, 1987.

Hypoxia Affects Tumor Cell Invasiveness In Vitro:

The Role of Hypoxia-Activated Ligand HAL1/13 (Ku 86 autoantigen).

Irene Ginis[2] and Douglas V. Faller[1]

[1] Cancer Research Center, and Departments of Medicine, Biochemistry, Pediatrics, Microbiology, Pathology and Laboratory Medicine, Boston University School of Medicine, Boston, MA 02118

and

[2] Stroke Branch, National Institute of Neurological Disorders and Stroke, NIH, Bethesda MD 20892

Running title: hypoxia effect on tumor cell invasiveness

Key words: hypoxia, tumor cells, invasion, metastasis, adhesion molecules

Address correspondence to:
Irene Ginis, M.D., Ph.D.
Senior Staff Fellow
Stroke Branch, NINDS, NIH
Building 36, Room 4A03
Bethesda, MD 20892-4128

Tel: 301-435-7655
FAX: 301-402-2769
Email: ginis@codon.nih.gov

ABSTRACT

Multiple studies demonstrate that tumor cells which have recovered from hypoxic exposure exhibit higher metastatic potential. Hypoxia is also known to induce extravasation of leukocytes during ischemic injury. We have recently identified and characterized a new adhesion ligand, HAL1/13 (Hypoxia-Activated Ligand), which mediates the increase in leukocyte adhesion to endothelium under hypoxic conditions (J. Immunol. 155: 802-810, 1995). The HAL1/13 antigen was cloned and found to be identical to p86 subunit of Ku autoantigen. HAL1/13/Ku86 was shown to be expressed on the surface of several leukemic cell lines and of rhabdomyosarcoma cells, as well as normal endothelial cells after hypoxic exposure. In this study we demonstrate that the HAL1/13 antigen is expressed on the surface of neuroblastoma (Kelly) and breast carcinoma (MCF-7) cells. Furthermore, hypoxic exposure of neuroblastoma and breast carcinoma cells resulted in upregulation of HAL1/13 surface expression, coincident with an increased ability of these tumor cells to invade endothelial monolayers. This enhanced invasion could be partially attenuated by the anti-HAL1/13 antibody. Hypoxia also potentiated neuroblastoma and breast carcinoma cell transmigration through Matrigel filters, although their haptotactic locomotion on laminin was not affected. Anti-HAL1/13 antibody inhibited locomotion of hypoxic tumor cells on laminin. These studies indicate that HAL1/13/Ku86 antigen mediates, in part, the increased invasiveness of tumor cells induced by hypoxia, as well as the adhesion of normal leukocytes to hypoxic endothelium.

INTRODUCTION

Endothelial cells from different sources, as well as rhabdomyosarcoma (RD) cells, increase their adhesiveness for leukocytes when subjected to hypoxic treatment (12, 13). In a functional screen of antibodies generated against membrane antigens on hypoxic RD cells, we have identified and characterized a new cell surface molecule, HAL1/13 (Hypoxia-Activated Ligand), which is expressed on both endothelial and RD cells, and which we have shown to mediate the increased adhesion of leukocytes under hypoxic conditions (15).

In 1997, we identified the HAL1/13 antigen by expression cloning (16). The HAL1/13 antigen was found to be identical to p86 subunit of the DNA-binding protein, Ku, previously identified as a target for autoantibodies produced by patients with systemic lupus erythematosus and related rheumatic disorders (17), and as a regulatory subunit of the DNA-dependent protein kinase (Han et al., 1996). In addition, commercial antibodies raised against Ku86 recognized the HAL1/13 antigen. Although Ku86 was initially thought to be a nuclear antigen, Ku86 has been recently found on the surface (18-20), and in the cytoplasm (Fewell and Kuff , 1996), of certain cell types. More recent results from our laboratory have confirmed the ability of hypoxia to induce translocation of HAL1/13-Ku86 from the nucleus to the plasma membrane. Furthermore, we have shown that transfected HAL1/13-Ku86 localizes to the plasma membrane of NIH-3T3 cells, and enhances the adhesion of lymphocytes to these transfected cells (E. Lynch, R. Moreland, I. Ginis, and D.V. Faller, manuscript in preparation).

Although the HAL1/13 antigen did not cluster with known leukocyte antigens, some leukemic cell lines, including Jurkat, Molt-4, HL-60 and U937, reacted strongly with the anti-HAL1/13 antibody (15). With the exception of rhabdomyosarcoma (RD) cells, solid tumor cell lines have not been tested for the expression of HAL1/13. In this paper, we have studied the effect of hypoxia on two other solid tumor cell lines, neuroblastoma (Kelly) and breast carcinoma (MCF-7) cells, which express HAL1/13-Ku86 on their surface. We present evidence that when these cells are exposed to low oxygen environments, their ability to invade endothelial cell monolayer and to transmigrate through Matrigel-coated filters is increased, and surface expression of HAL1/13-Ku86 is upregulated. Our results suggest that HAL1/13-Ku86 plays a major role in regulating the invasive potential of tumor cells.

MATERIALS AND METHODS

Cell Cultures: Human umbilical vein endothelial cell (HUVEC) cultures have been previously described (13). Early passages (4-6) of endothelial cells were grown to confluence on 10 cm cell culture dishes, then trypsinized, washed and plated at high density (approximately 5 x 10^5 cells/well) onto gelatin-coated 96 well microtiter plates (Nunclon, Denmark). These cultures attained confluence 24-48 hours later and were used in adhesion experiments. Neuroblastoma Kelly cells were obtained from the tissue culture facilities of the University of California, San Francisco. Breast carcinoma cells (MCF-7) were obtained from the American Type Culture Collection (Rockville, MD). Both cell lines were grown in Dulbecco Modified Eagle's Medium (DMEM) supplemented with 10% Fetal Calf Serum (FCS) (Sigma, St. Louis), 2 mM L-glutamine, 100 units/ml of penicillin and 100 µg/ml of streptomycin (Gibco Laboratories, Grand Island, NY) at 37°C in a 5% CO_2 atmosphere.

Hypoxic Treatment of Tumor Cells: Subconfluent tumor cell cultures were covered with 5 ml fresh culture medium (DMEM/10% FBS), containing 20 mM HEPES to prevent a pH drop during hypoxic exposure. The plates were placed in modular incubator chambers (Billups Rothenberg, Del Mar, CA) and flushed with a 5% CO_2/95,% N_2 gas mixture for 30 min. Chambers were agitated every 5 min to insure maximal gas exchange in the culture medium. Oxygen concentration in the culture medium was monitored with an oxygen meter (Microelectrodes, Inc., Bedford NH) and reached 10 torr at the end of treatment. The chambers were sealed and incubated for various time intervals at 37° C. Incubation of tumor cells under these hypoxic conditions had no significant effect on their viability: greater than 90% of cells

were alive at the end of incubation as assessed by trypan-blue exclusion. Cells continued to proliferate after reoxygenation.

Flow Cytometry: Cells were trypsinized, washed with phosphate-buffered saline (PBS) containing 0.5% bovine serum albumin and then incubated with the monoclonal antibody directed against HAL1/13 (15) for 40 min at 4°C in polystyrene round-bottom, 96-well plates. The cells were then washed and stained at 4°C for 40 min with a 1:25 dilution of FITC-conjugated $F(ab')_2$ sheep anti-mouse antibodies (Organon Teknika Corporation; Westchester, PA). The cells were fixed in 1% paraformaldehyde/PBS and analyzed on a Becton-Dickinson FACScan flow cytometer (San Jose, CA).

Adhesion Centrifugation Assays were performed as described in detail elsewhere (12, 13). Briefly, normoxic and hypoxic tumor cells were trypsinized, loaded by incubation in 2 μM of the fluorescent dye 2',7'bis(carboxyethyl)-5-(and -6) carboxy-fluorescein acetoxy methyl ester (Calcein) (Molecular Probes, Eugene, OR), and resuspended at $5x10^6$/ml in normoxic DMEM/10% FCS. Calcein-labeled tumor cells were added to 96-well plates coated with confluent monolayers of endothelial cells, in a volume of 100 μl/well. Plates were then incubated for 30 min at 37°C in a 5% CO_2 humidified incubator. In antibody-blocking experiments, the anti-HAL1/13 antibody was added to the tumor cell suspension just before plating. The fluorescence intensity of plated cells was read on a CytoFluor 2300 Plate Scanner (Millipore, Burlington, MA) at excitation and emission wavelengths of 485 and 530 nm, respectively. The plates, along with adherent cells, were sealed with transparent plastic (Dynatech Inc., Alexandria, VA), inverted and centrifuged at 100 x g, and the fluorescence of the

remaining adherent cells was read again and compared to initial fluorescence. Background fluorescence was measured separately for each plate and subtracted from all readings. Each experiment was performed in triplicate. The SD of repetitive readings was less than 30% of the mean.

Endothelial Cell Monolayer Invasion Assay: The assay was adopted from La Reviere et al. (21) and modified for quantitative measurements of invading cells using a Fluorescent Plate Reader. The method is based on the observation that the endothelial cell monolayer shields fluorescent-labeled tumor cells from the fluorescence detector, which is located beneath the plate. In order to quantitate the fluorescence-shielding factor, equal numbers of fluorescent beads or fluorescent-labeled cells were plated either onto uncoated wells of 96-well microtiter plate or onto wells coated with a confluent monolayer of endothelial cells. The plate was spun at 500 rpm for 5 min. to insure equal sedimentation of the beads or the cells onto the plate. The signals detected from the beads in both cases were compared. The fluorescent signal from the beads shielded by the endothelial cell monolayer was lowered by 16.17% compared to that of the beads plated directly onto the bottom of the well (334 ± 28 *vs* 402 ± 26 fluorescent units) (mean$\pm$SD; n=3, $p<0.01$). Based on this observation, the fluorescent signal of an invading tumor cell ($\mathbf{f}_{inv}$) would be 1.16 of the signal of a plated cell sitting on top of the endothelial monolayer ($\mathbf{f}_{pl}$):

$$\mathbf{f}_{inv} = 1.16 \times \mathbf{f}_{pl} \qquad (1)$$

The fluorescence of plated cells before initiation of invasion ($\mathbf{F}_o$) could be calculated as:

$$\mathbf{F}_o = \mathbf{N} \times \mathbf{f}_{pl} \qquad (2)$$ (where $\mathbf{N}$ is the number of plated cells)

Similarly, the fluorescence of tumor cells (**F**), measured at the end of co-incubation with the monolayer, could be calculated as a sum of the fluorescence of the invading cells (**F**inv) and of those which remained on the apical surface of the endothelium, (**F**ap), where:

Finv = (**N**inv x 1.16**f**pl) (3), where **N**inv is the number of invading cells;

Fap = (**N**-**N**inv)fpl (4)

F = **F**ap + **F**inv (5)

The percentage of invading cells (**N**inv/**N**) could be calculated based on equations 1-5:

$$\% \text{ invading cells} = 100 * \frac{F - d * Fo}{0.16 * d * Fo}$$

(where *d* is the dimming coefficient of the dye, which was found to be between 0.75 and 0.85 and was measured in each experiment).

Each experiment was performed in triplicate. The SD of repetitive readings was less than 30% of the mean.

Double Chamber Transmigration Assay: 6.5 mm filter inserts for 24-well plates (Costar Corporation, Cambridge, MA) with a pore size large enough to be penetrated by tumor cells (8 μm) were incubated overnight with 70 μl of a 1:50 dilution (0.2 mg/ml) of a reconstituted basement membrane solution (Matrigel, Becton Dickinson), at room temperature. Tumor cells exposed to normoxic or hypoxic environments were trypsinized, counted, and resuspended at $2x10^6$ cells/ml in culture medium, and then plated onto filter inserts in a volume of 100 μl. 1 ml of culture medium conditioned by normoxic tumor cells was added in lower chambers. The cells plated onto inserts were incubated at 37°C in a 5% CO_2 humidified atmosphere for 24 hours.

The inserts were then removed and those cells which had migrated into the lower chamber were labeled with calcein (final concentration 2 μM, 30 min. at 37°C), and their fluorescence (**F**migrated) was read with a CytoFluor 2300 Plate Scanner. In parallel experiments, the same number of cells were plated directly onto the bottom of 24 well plates with no inserts. These wells were immediately incubated with the fluorescent dye, calcein, and the cell fluorescence (**F**plated) was measured using a Fluorescent Plate Reader. The percentage of transmigrating cells was calculated as:

% migrating cells = **F**migrated/**F**plated x 100

Cell Motility Studies: Cell motility was measured by time lapse videomicroscopy according to the method of Echtermeyer et al. (22). Tumor cells were subjected to hypoxia for 24 or 48 hours and resuspended at 10^6/ml in DMEM. A small aliquot (50-100 μl) of the tumor cell suspension was plated into 1 ml of pre-warmed DMEM on a 35 mm tissue culture dish which had been pre-coated with laminin (by exposure to a 10 μg/ml solution for 2 hours at room temperature, and then washed twice with PBS). The dish was placed on the microscope table, and tumor cells were allowed to settle for 10 min before the start of videorecording. The temperature in the plastic hood covering the microscope was maintained at 37°C during the entire recording period (16-20 min). The image of the microscopic field was captured every minute, yielding 16-20 images for each sample. Coordinates of single cells in a series of images were measured using NIH Image software. The migration of 15-18 randomly-selected cells per field was analyzed.

Statistical Analysis was carried out by means of the paired "Student's" t-Test.

Blank

RESULTS

Neuroblastoma (Kelly) and breast carcinoma (MCF-7) cells express the HAL1/13 antigen, and its expression is upregulated during hypoxic exposure.

The results of flow cytometric analysis of normoxic neuroblastoma and breast carcinoma cells stained with anti-HAL1/13 antibody are presented on **Figure 1**A and C respectively. Both cell lines were found to constitutively express HAL1/13. Incubation of these cells in hypoxic environments for 24-48 hours resulted in consistent upregulation of HAL1/13 expression on their surface. In neuroblastoma Kelly cells, the maximum effect of hypoxic treatment was observed at 24 hours (Fig. 1B); incubation of the cells in the hypoxic chambers for 48 hours did not further increase HAL1/13 expression (data not shown). Similar experiments in MCF-7 cells demonstrated a time-dependent increase of HAL1/13 expression, with maximum expression at 48 hours (Fig. 1D).

Hypoxia stimulates tumor cell invasion of an endothelial cell monolayer.

We next determined whether hypoxia-induced expression of HAL1/13 on neuroblastoma and breast carcinoma cells affects their interactions with endothelial cells. We hypothesized that hypoxic tumor cells might become more invasive as a result of Hal1/13 induction. This hypothesis was tested by means of two *in vitro* techniques: a monolayer invasion assay, and confocal microscopy. Tumor cells, loaded with fluorescent dye, were allowed to adhere to endothelium for 30 min and non-adherent cells were then washed out. The remaining adherent tumor cells were left on the endothelial monolayer for additional 4 hours. During this period, some of the tumor cells invaded into the endothelial monolayer and diapedesed beneath it. The

invading cells were brought into closer proximity to the fluorescence detector, which we determined to result in a 16% increase in the fluorescence signal detected by the fluorescent plate reader (see *Methods* for calculations and formulae). Having determined this empirical coefficient relating the fluorescence of adherent tumor cells before and after invasion, it was possible to calculate the percentage of invading cells. The results of these experiments are presented in **Figure 2**. Only a small percentage (5.2%) of normoxic Kelly neuroblastoma cells were able to invade an endothelial cell monolayer. After a 24 hour incubation under hypoxic conditions, however, the fraction of invading tumor cells dramatically increased to 54.3% (n=7; p=0.001). As shown in Figure 2A, the anti-HAL1/13 monoclonal antibody partially inhibited the ability of hypoxic Kelly cells to invade endothelium, with the percentage of invading cells dropping to 27.8% (n=5; p=0.026). No additional increase in invasive potential was observed in neuroblastoma cells when the hypoxic exposure was extended to 48 hours (53.1%; n=4). In contrast, hypoxic exposure of MCF-7 cells resulted in a time-dependent increase in invasiveness, from 11.3% in control cells to 47.06% in tumor cells subjected to 24 hours of hypoxia (n=5; p=0.012), and to 70.9% after 48 hours of exposure to hypoxia (n=5 p=0.01). The antibody against HAL1/13 inhibited invasion of MCF-7 cells subjected to 24 and 48 hours of hypoxia, to 22.3% (n=6; p=0.05) and 34.7% (n=5; p=0.01) respectively (Fig.2B). Thus, these assays correlated the hypoxia-activated invasive potential of tumor cells with the temporal course of HAL1/13 induction by hypoxia, and showed that this invasiveness is dependent in large part upon the presence of HAL1/13.

The results of the invasion assay did not depend on the ability of tumor cells to adhere to endothelial cells. The data presented in Table 1 demonstrate that hypoxic exposure did not

increase adhesion of either neuroblastoma or breast carcinoma cells to endothelial cells. In fact, both tumor cell lines exhibited significantly decreased adhesion to endothelium after 24 and 48 hours of hypoxic treatment, respectively. The monoclonal antibody directed against HAL1/13 had no effect on tumor adhesion to endothelium (**Table 1**).

To confirm the results of the invasion assay, neuroblastoma (Kelly) cell invasion of endothelial cells was monitored by fluorescent confocal microscopy. Kelly cells were subjected to hypoxia for 48 hours, loaded with the fluorescent dye (calcein) and co-incubated with confluent monolayers of endothelial cells for 4 hours. The monolayer was scanned on 5 different levels, 4 μm apart. Figure 3A represents a microphotograph of normoxic Kelly cells taken on the level 4 (17 μm from the top of the monolayer). Essentially no cells were seen at this level, under these conditions. Microphotography of Kelly cells previously exposed to hypoxia, however, taken at the same scanning level, demonstrated the presence of a significant number of invading cells (Fig. 3B)

Hypoxia alters tumor cell interactions with extracellular matrices.

The effect of hypoxia on the ability of the tumor cells to cross basement membranes and migrate along extracellular matrices (ECM) was tested in a transmigration assay using polycarbonate filters coated with Matrigel mixture of ECM proteins. The results of these studies are presented in **Figure 4**. The neuroblastoma cells were able to traverse Matrigel-coated membranes more efficiently when first subjected to hypoxia for 24 hours (30.7 *vs* 22.7%, n=3 p=0.034). Baseline (normoxic) transmigration of breast carcinoma MCF-7 cells was lower than that of neuroblastoma cells, but hypoxic exposure had a demonstrable effect on these cells as

well, increasing their migration through the Matrigel-coated filters from 5.5% to 10.7 % (n=3; p=0.002).

We next determined whether the effect of hypoxia on tumor cell migration through ECM was associated with increased cell motility. Using computerized videomicroscopy, the locomotion of Kelly or MCF-7 cells on a laminin-coated surface was traced. The results of one such experiment are illustrated in Figure 5A. Four MCF-7 cultures were subjected to 4 different treatments (normoxia or hypoxia, with or without subsequent treatment with anti-HAL1/13 antibody), and plated onto 4 tissue culture dishes coated with laminin. The movements of 15-16 cells in each field were recorded by videomicroscopy, with images captured every minute for 16 min thus producing 4 sets of 16 images. **Figure 5**A illustrates the actual distances in pixels (1 pixel=1μm) migrated by each individual cell. The horizontal bars indicate the mean distances traversed for each type of treatment. Figure 5B is a summary of the results of 3-4 such experiments for each tumor cell line. There was no effect of hypoxia on the motility of Kelly or of MCF-7 cells on laminin. Pretreatment of hypoxic tumor cells with the anti-HAL1/13 antibody for 1 hour before plating on laminin, however, resulted in a decrease of mean migration distances (19.4% for Kelly cells, and 15.6% for MCF-7 cells; p=0.004 for both cell lines) (Fig. 5B). The anti-HAL1/13 antibody had no effect on the motility of normoxic tumor cells.

DISCUSSION

It has been known for many years that tumor oxygenation plays a significant role in responsiveness to radiation (23) and to anti-tumor drug therapy (24), and in the formation of metastases (25). Similarly, *in vitro* studies have demonstrated that tumor cells which have recovered from hypoxic exposure exhibit higher metastatic potential. Thus, cells isolated from hypoxic regions of murine tumors have been shown to have an increased lung colonization capability (26). Similarly, exposure to hypoxia for 24 hours, followed by 18 hours of reoxygenation, resulted in 14-fold and 6-fold increases in the lung colonization potential of fibrosarcoma and melanoma cells, respectively (27). Another study demonstrated that 24-48 h recovery from acidosis or glucose starvation resulted in a marked (30-fold) increase in metastatic ability (28). Successive cycles of exposure to severe hypoxia up to 72 hours, or to mild hypoxia up to 12 days, followed by growth to confluence for several weeks, permitted emergence of metastatic variants from a non-metastatic clone of B16 melanoma (29).

The molecular events leading to this metastatic phenotype of hypoxic tumor cells remain poorly understood, however. Young, et al. demonstrated DNA over-replication in anaerobic culture of fibrosarcoma and melanoma cells after reoxygenation (27). Hypoxia was reported to induce upregulation of cancer-related VL30 elements (30) and c-*jun* (31-33) and c-*fos* (16, 34, 35). Enhanced synthesis of so-called oxygen-regulated proteins, or ORP, has been observed in a variety of rodent and human tumor cell lines exposed to low oxygen levels (36). Although the role of tumor cell interactions with endothelium and extracellular matrices in the development of

tumor metastases is well-documented, the effect of hypoxia on tumor adhesion receptors has not been studied.

In this report, we demonstrate that neuroblastoma and breast carcinoma cells, when subjected to low oxygen environments, increase their ability to invade endothelial cells *in vitro*. While neuroblastoma or breast carcinoma cells previously exposed to ambient oxygen concentrations remained adherent to the apical surface of endothelial cells during the entire period of observation (4 hours), those same cells, if previously exposed to hypoxic conditions for 24-48 hours, acquired the ability to move through the monolayer. Cell movement through the monolayer was also monitored with confocal microscopy, and this assay confirmed that the majority of normoxic cells could be detected at the endothelial surface, while hypoxic tumor cells invaded through the monolayer and resided at the bottom. A more invasive phenotype of hypoxic tumor cells correlated with overexpression of HAL1/13, an endothelial cell surface molecule, which has been recently reported to contribute to hypoxia-induced interactions of endothelial cells (15) with leukocytes and later has been identified as the p86 subunit of Ku-antigen (16).

Epithelial-like MCF-7 cells have been previously classified as intermediate filament protein, vimentin (VM)-positive and estrogen receptor (ER)-negative. They form no colonies in Matrigel, exhibit no chemotaxis, and do not metastasize in nude mice (37). Initially non-invasive MCF-7 cells, which expressed high levels of HAL1/13 even before hypoxic exposure, responded to hypoxic environments by further upregulation of HAL1/13 and demonstrated increased invasiveness of endothelial cells. In contrast, MDA-MB-231 and Hs578T fibroblastoid cell lines

represent a group of ER^-/VIM^- cells, and have been shown to form colonies in Matrigel outgrowth assay, to be more invasive in the Boyden chamber chemoinvasion assay, and to metastasize in nude mice. These cell lines exhibited high invasiveness even before hypoxic treatment, and we were thus unable to detect any hypoxia-induced augmentation of invasiveness in our assay (data not shown). These observation suggest that tumor cell invasion depends upon multiple factors, with HAL1/13-Ku86 playing a role. Indeed, hypoxia-induced invasiveness of neuroblastoma and breast carcinoma cells was only partially inhibited by HAL1/13 antibodies.

ECM-degrading enzymes such as collagenase type IV and other metalloproteinases might play a role here. We have recently shown that exposure to hypoxia upregulates collagenase type IV (MMP-9) transcription and enzymatic activity in endothelial cells (32) [although similar experiments in ovarian carcinoma cell lines demonstrated either no hypoxia-induced increase of metalloproteinase activity (40), or if such an increase was observed, no correlation with the metastatic potential of the tumor cells (41, 42)]. Hypoxia was shown to upregulate the levels of cathepsin (L+B) in murine sarcoma cells and increase their invasion of Matrigel filters (Cuvier). In this study we have investigated the effect of hypoxic environments on the ability of tumor cells to both traverse ECM-coated membrane and to migrate on laminin, a major component of basement membrane, which has been shown to promote locomotion of different types of cells including tumor cells (43). The two cell lines studied exhibited different abilities to transmigrate through a Matrigel filter, with Kelly more active than MCF-7, but both tumor cell lines demonstrated increased transmigration upon hypoxic exposure. No transmigration was observed if the medium in the bottom chamber was not conditioned by corresponding normoxic cells (or even other cell types), suggesting that transmigration of tumor cells studied in our experiments

was of chemotactic nature. Addition of medium conditioned by hypoxic tumor cells did not affect the outcome of the transmigration assay (data not shown), indicating that increased transmigration of hypoxic cells was not associated with the release of a new chemoattractant but rather with changes in cell migration mechanisms, such as expression of new adhesion receptors or cell movement machinery. However, non-directional movement of the tumor cells on laminin was not affected by hypoxia, at least in this assay, in which we have measured the sum of the distances which each cell migrated during 1 min intervals over 16-18 min of observation. [This method is limited to independent straight-line displacements and does not take into account locomotion at different angles between the measurements and cell rotation (44)]. One surprising finding was the inhibitory effect of the anti-HAL1/13 antibody on the motility of hypoxic tumor cells. While the antibody had no effect on normoxic tumor cells motility, it significantly inhibited haptotaxis of hypoxic Kelly and MCF-7 cells by 19.4% and 15.6%, respectively, suggesting perhaps a switch in the utilization of adhesion/locomotion molecules in these tumor cells in response to hypoxic exposure.

Interaction of tumor cells with ECM is particularly important at the last stage of the metastatic process, when blood-borne tumor cells transmigrate through the subendothelial basement membrane and colonize the target organs. The effectiveness of this process depends on interplay of different adhesion forces, on one hand allowing tumor cell movement along the ECM, and on the other hand, trapping the cell at the site of metastasis. Interestingly, exposure of neuroblastoma or breast carcinoma cells to hypoxic environments caused no significant increase but rather a decrease, in their adhesion to endothelium. Decreased adhesion of hypoxic tumor cells to endothelium was paralleled by decreased adhesion of tumor cells to each other. On

average, 68.1± 1.0% (mean ± SD) of Kelly cells were able to withstand centrifugation force of 28 x g, and remained adherent to a monolayer of the same cells. Kelly cells subjected to hypoxia for 24 hours, however, decreased their adhesiveness to a confluent normoxic monolayer of Kelly cells by 2 fold (28.3± 4.1%; p=0.035) (Ginis, unpublished observations). Similarly, Hasan et al. (38) observed detachment of hypoxic human melanoma cells from ECM, associated with downregulation of integrin receptors and CD44 and N-CAM. In reciprocal experiments, overexpression of the fibronectin receptor in melanoma cells inhibited Matrigel invasion and pulmonary metastasis by the transfectants (39).

Although the nuclear protein Ku86 has been studied in connection with DNA repair and replication, recent observations demonstrate a role for Ku86 as a surface protein (18, 19) and a participation in cell-cell interactions (20). The p86 subunit of the Ku antigen was identified as a somatostatin receptor (distinct from the seven-transmembrane domain receptor), which regulates activity of phosphatase-2A (Le Romancer). Somatostatin and its analogs have been implicated in the translocation of Ku86 to the nucleus in cancer cells (Tovari) and in the modulation of adhesion of leukocytes (Leszczynski) and cancer cells (Gastpar) to endothelium. Involvement of somatostatin receptors in multiple signaling events, such as decreases of intracellular levels of cAMP, decreases in intracellular Ca^{2+} and PKA activity, and others (for the recent review see Patel) suggests the possibility that surface Ku86 could also control cell adhesion and migration of cancer cells, by transducing signals into a cell which cause cytoskeletal changes and/or changes of affinity of adhesion receptors. Our recent demonstration that transfection and ectopic expression of (human) HAL1/13-Ku86 on (murine) NIH-3T3 fibroblasts confers the ability of these normally non-adhesive cells to bind to a variety of human lymphoid cell lines, and this

adhesion can be specifically blocked by HAL-1/13-neutralizing antibodies, confirms the ability of HAL1/13-Ku86 to function as an adhesion molecule cells (E. Lynch, R. Moreland, I. Ginis, and D.V. Faller, manuscript in preparation). The etiology of the high level of membrane localization of HAL1/13-Ku86 in tumor cells, and the mechanisms underlying its adhesive function, are under investigation. Our recent findings demonstrate that upregulation of HAL1/13-Ku80 expression at the cell surface is mediated by translocation of the antigen from the nucleus.

In Summary, these studies indicate that the HAL1/13-Ku86 molecule may mediate, in part, the increased invasiveness of tumor cells induced by hypoxia, as well as regulating hypoxia-induced adhesion of normal lymphocytes and leukocytes to endothelial cells.

Acknowledgments:

This work was supported in part by grants from the Department of the Army (RP-951255) (DVF) and from NIH/NIAID P60AR20613 (DVF).

We want to thank by Dr. Vickery Trinkaus-Randall, Biochemistry Department, Boston University School of Medicine for her help with confocal microscopy, Dr. Carolyn Smith (NINDS, NIH) for her assistance with videomicroscope, and Dr. Inna Goldfarb (NCI, NIH) for her assistance with HAL1/13 hybridoma culture.

REFERENCES

1. Schirrmacher, V. Cancer metastasis: Experimental approaches, theoretical concepts, and impacts for treatment strategies. *Adv Cancer Res*, 43:1-73, **1985**

2. Roos, E, La Riviere, G, Collard, JC, et al. Invasiveness of T cell hybridomas in vitro and their metastatic potential in vivo. *Cancer Res*, 45:6238-6243, **1985**

3. Kubes, P. Polymorphonuclear leukocyte-endothelium interactions: a role for pro-inflammatory and anti-inflammatory molecules. *Can. J. Physiol. Pharmacol.* 71:88-97, **1993**

4. Dejana, E., Bertocchi, F., Bortolami, M.C., Regonesi, A, Tonta, A., Breviario, F., and Giavazzi, R. Interleukin-1 promotes tumor cell adhesion to cultured human endothelial cells. *J Clin Invest*, 82:1466-1470, **1988**

5. Rice, G.E., Gimbrone, M.A., Jr., and Bevilacqua, M.P. Tumor cell-endothelial interactions: increased adhesion of human melanoma cells to activated vascular endothelium. Am. J. Pathol., 133:204-210, **1988**

6. Bereta, M., Bereta, J., Cohen S., Zaifert, K., Cohen, M.C. Effect of inflammatory cytokines on the adherence of tumor cells to endothelium in a murine model *Cell Immunol*, 136:263-277, 1991

7. Okahara, H., Yagita, H., Miyake, K. and Okumura, K. Involvement of very late activation antigen 4 (VLA-4) and vascular cell adhesion molecule-1 (VCAM-1) in tumor necrosis factor a enhancement of experimental metastasis. *Cancer Res,* 54:3233-3236, **1994**

8. Zetter, B.R. Adhesion molecules in tumor metastasis. Seminars in Cancer Biol, 4:219-29, **1993**

9. La Riviere, G., Gebbinc, J.W.T.M.K., Driessens, M.H.E., and Roos, E. Pertussis toxin inhibition of T-cell hybridoma invasion is reversed by manganese-induced activation of LFA-1. *J Cell Sciences*, 107:551-559, **1994**

10. Sawada, R., Tsuboi, S., Fukuda, M. Differential E-selectin-dependent adhesion efficiency in sublines of a human colon cancer exhibiting distinct metastatic potentials. *J Biol Chem*, 269:1425-1431, **1994**

11. Zocchi, M.R. and Poggi, A. Lymphocyte-endothelial cell adhesion molecules at the primary tumor site in human lung and renal cell carcinomas. *J.Natl cancer Inst* 85:246-247, **1993**

12. Ginis, I, S.J. Mentzer, and D.V. Faller. Hypoxia induces lymphocyte adhesion to human mesenchymal cells via an LFA-1-dependent mechanism. *Am.J. Physiol.* 264 (3), part1: C617-C624, **1992**

13. Ginis, I, S.J. Mentzer, and D.V. Faller. Oxygen tension regulates neutrophil adhesion to human endothelial cells via an LFA-1-dependent mechanism. *J. Cell Physiol* 157:569-578, **1993**

14. Brizel, D.M., Scully, S.P., Harrelson, J.M., Layfield, L.J., Bean, J.M., Proznitz, L.R., and Dewhirst, M.W. Tumor oxygenation predicts for likelihood of distant metastases in human soft tissue sarcoma. *Cancer Research*, 56:941-943, **1996**

15. I. Ginis, Mentzer S.J., and Faller, D.V. Characterization of a hypoxia-responsive adhesion molecule for leukocytes on human endothelial cells. *J. Immunology*, 155: 802-810, **1995**

16. Faller, D.V. Hypoxia, Nitric Oxide and Vasoactive Gene Transcription. In: Nitric Oxide, Cytochrome P450 and Sexual Steroid Hormones. J. Parkinson, ed. **1997.** Springer-Verlag, New York, pp.75-116.

17. Reeves, W.H., Antibodies to the p70/p80 (Ku) antigens in systemic lupus erythematosus. *Rheumatic Diseases Clinics of North America*, 18(2):391-414, **1992**.

18. Dalziel, RG, Mendelson, S.C., Quinn, J.P. The nuclear autoimmune antigen Ku is also present on the cell surface. *Autoimmunity*;13(4):265-267, **1992**

19. Prabhakar, B.S., Allaway, G..P, Srinivasappa, J., Notkins, A.L. Cell surface expression of the 70-kD component of Ku, a DNA-binding nuclear autoantigen. *J Clin Invest.* 86(4):1301-1305, **1990**

20. Teoh, G., Urashima, M., Greenfield, E.A., Nguyen, K.A., Lee, J.F., Chauhan, D., Ogata, A., Treon, S.P., Anderson, K.C.. **1998**. The 86-kD subunit of Ku autoantigen mediates homotypic and heterotypic adhesion of multiple myeloma cells. *J Clin Invest*,101(6):1379-1388

21. La Reviere, G., Schipper, C.A., Collard, J.G. and Roos, E. Invasiveness in hepatocyte and fibroblast monolayers and metastatic potential of T-cell hybridomas in mice. *Cancer Res*, 48:3405-3410, **1988**

22. Echtermeyer, F., Schober, S., Poschl, E., von der Mark, H., and von der Mark, K. Specific induction of cell motility on laminin by α7 integrin. *J. Biol Chem*, 272 (26):2071-2075, **1996**

23. Chapman JD, Engelhardt EL, Stobbe CC, Schneider RF, Hanks GE. 1998. Measuring hypoxia and predicting tumor radioresistance with nuclear medicine assays. *Radiother Oncol*, 46(3):229-37

24. Brown JM . 1990. Tumor hypoxia, drug resistance, and metastases. *J Natl Cancer Inst*, 82(5):338-9

25. Dachs GU, Chaplin D. 1998. Microenvironmental control of gene expression: implications for tumor angiogenesis, progression, and metastasis. *Semin Radiat Oncol*, 8(3):208-16

26. Young, S., Hill, R.P. Effects of reoxygenation on cells from hypoxic regions of solid tumors: anti-cancer drug sensitivity and metastatic potential. *J Natl Cancer Inst*, 82:371-380, **1990**

27. Young, S.D., Marshall, R.S., and R.P. Hill. Hypoxia induces DNA overreplication and enhances metastatic potential of murine tumor cells. *Proc Natl Acad Sci USA*, 85:9533-9537, **1988**

28. Schlappack O.K., Zimmermann, A., and Hill, R.P. Glucose starvation and acidosis: effect on experimental metastatic potential, DNA content and MTX resistance of murine tumor cells. *Br J Cancer*, 64:663-670, 1991

29. Stackpole, C.W., Groszek L., Kalbag, S.S. Benign to malignant B16 melanoma progression induced in two stages in vitro by exposure to hypoxia *J. Natl. Cancer Inst.* 86:361-367, **1994**

30. Anderson, G.R., Stoler, D.L., and Scarcello, L.A. Retrotransposon-like VL30 elements are efficiently induced in anoxic rat fibroblasts. *J Mol Biol*, 205:765-769, **1989**

31. Ausserer, W.A., Bourrat-Floeck, B., Green, C.J., Laderoutr, K.R., and Sutherland, R.M. Regulation of c-jun expression during hypoxic and low-glucose stress. *Molec and Cell Biol,* 14:5032-5042, **1994**

32. Bandyopadhyay R.S., Phelan M., and Faller D.V. Hypoxia induces AP-1-regulated genes and AP-1 transcription factor binding in human endothelial and other cell types *Biochim Biophys Acta*;1264(1):72-78, **1995**

33. Bandyopadhyay, R.S. and Faller, D.V. Regulation of c-*jun* gene expression by hypoxia in endothelial cells. 1997, *Endothelium*, 5:95-106. **1997**

34. Muller, J.M., Krauss, B., Kaltschmidt, C., Baeuerle, P.A., and Rupec, R.A. Hypoxia induces c-fos transcription via mitogen-activated protein kinase-dependent pathway. *J. Biol Chem*, 272(37):23435-23439, **1997.**

35. Faller, D.V. Endothelial Cell Responses to Hypoxic Stress. *Clinical and Experimental Pharmacology and Physiology,* 26:74-84, **1999**

36. Heacock, C.S. and Sutherland, R.M. Enhanced synthesis of stress proteins caused by hypoxia and relation to altered cell growth and metabolism. *Br J Cancer,* 62:217-225, **1990**

37. Thompson, E.W., Paik, S. Brunner, N. et. al. Association of increased basement membrane invasiveness with absence of estrogen receptor and expression of vimentin in human breast cancer cell lines. *J. Cell Physiol.* 150:534-544, **1992**

38. Hasan, N.M., Adams, G.E., Joiner, M.C., Marshall, J.F., and Hart, I.R. Hypoxia facilitates tumor cell detachment by reducing expression of surface adhesion molecules and adhesion to extracellular matrices without loss of cell viability. *Br J Cancer*, 77(11):1799-1805, **1998**

39. Qaian, F., Vaux, D.L., and Weissman, I.L. Expression of the integrin a4b1 on melanoma cells can inhibit the invasive stage of metastasis formation. *Cell*, 77:335-347, **1994**

40. Krtolica, A. and Ludlow, J.W. Hypoxia arrests ovarian carcinoma cell cycle progression, but invasion is unaffected. *Cancer Res*, 56:1168-1173, **1996**

41. Jang, A. and Hill, R.P. An examination of the effects of hypoxia, acidosis, and glucose starvation on the expression of metastasis-associated genes in murine tumor cells. *Clin Exp Metastasis*, 15(5):469-483, **1997**

42. Himelstein, B.P., and Koch, C.J., Studies off type IV collagenase regulation by hypoxia. *Cancer Lett*, 124(2):127-133), **1998**

43. Rabinovitz I., Mercurio A.M. The integrin alpha6beta4 functions in carcinoma cell migration on laminin-1 by mediating the formation and stabilization of actin-containing motility structures. *J Cell Biol*; 139(7):1873-1884, **1997**

44. Nossal, R. and Weiss, G.H. A descriptive theory of cell migration on surfaces. *J Theor Biol*, 47:103-113, **1974**

45. Sheetz M.P., Felsenfeld D.P., Galbraith C.G. Cell migration: regulation of force on extracellular-matrix-integrin complexes. *Trends Cell Biol*;8 (2):51-54, **1998**

46. Fewell JW, Kuff EL .Intracellular redistribution of Ku immunoreactivity in response to cell-cell contact and growth modulating components in the medium. J Cell Sci 1996 109 (Pt 7):1937-1946

47. Han Z, Johnston C, Reeves WH, Carter T, Wyche JH, Hendrickson E. Characterization of a Ku86 variant protein that results in altered DNA binding and diminished DNA-dependent protein kinase activity. J Biol Chem 1996 271:14098-14104

48. Cuvier C, Jang A, Hill RP Exposure to hypoxia, glucose starvation and acidosis: effect on invasive capacity of murine tumor cells and correlation with cathepsin (L + B) secretion. Clin Exp Metastasis 1997 Jan;15(1):19-25

49. Le Romancer M, Reyl-Desmars F, Cherifi Y, Pigeon C, Bottari S, Meyer O, Lewin MJ The 86-kDa subunit of autoantigen Ku is a somatostatin receptor regulating protein phosphatase-2A activity. J Biol Chem 1994 Jul 1;269(26):17464-8

50. Gastpar H, Zoltobrocki M, Weissgerber PWThe inhibition of cancer cell stickiness by somatostatin. Res Exp Med (Berl) 1983;182(1):1-6

51. Leszczynski D, Dunsky K, Josephs MD, Zhao Y, Foegh ML Angiopeptin, a somatostatin-14 analogue, decreases adhesiveness of rat leukocytes to unstimulated and IL-1 beta-activated rat heart endothelial cells. Life Sci 1995;57(15):PL217-23

52. Tovari J, Szende B, Bocsi J, Falaschi A, Simoncsits A, Pongor S, Erchegyi J, Stetak A, Keri G . A somatostatin analogue induces translocation of Ku 86 autoantigen from the cytosol to the nucleus in colon tumour cells. Cell Signal 1998 Apr;10(4):277-82

53. Patel YC . Somatostatin and Its Receptor Family. Front Neuroendocrinol 1999 Jul;20(3):157-198

Table 1. Effect of Hypoxia on Tumor Cell Adhesion to Endothelial Cells.

	control		**24 h hypoxia**		**48 h hypoxia**	
HAL1/13	-	+	-	+	-	+
Kelly (4)	37.7±6.9	37.7±8.1	25.5±5.3*	29.8±5.6	33.5±4.1	34.8±2.6
MCF-7 (7)	69.2±7.2	67.8±5.8	60.4±3.4	61.3±3.8	44.5±6.1*	52.5±6.6

Control tumor cells (normoxic) and cells subjected to hypoxia for 24 and 48 hours were allowed to adhere to endothelial cells monolayers for 30 min in the absence or presence of the HAL1/13 monoclonal antibody at 10 μg/ml. Percentage of adherent cells was quantitated as described in Methods. The data represents mean ± SEM, and the number of experiments performed with each tumor cell line is shown in parenthesis. Asterisks indicate statistically significant differences from the corresponding control value ($p<0.05$).

FIGURE LEGENDS.

Figure 1. The effect of hypoxia on HAL1/13 antigen expression on the surface of neuroblastoma and breast carcinoma cells. Neuroblastoma cells (Kelly - A and B) and breast carcinoma (MCF-7 - C and D) cells were fluorescently-immunostained with the monoclonal antibody directed against the HAL1/13 antigen. In windows A and C, histograms of normoxic cells stained with HAL1/13-specific antibodies are superimposed on histograms of corresponding cells stained with isotype-matched antibodies (TS1/18 [anti-CD18]). In windows B and D, histograms of cells exposed to hypoxia for 24 hours (Kelly, MCF-7) and for 48 hours (MCF-7) are superimposed on histograms of corresponding control, normoxic cells.

Figure 2. Effect of hypoxic exposure on tumor cell invasion of an endothelial monolayer. Kelly (A) and MCF-7 cells (B) were subjected to hypoxia, trypsinized, labeled with calcein, and coincubated with an endothelial monolayer for 4 hours, in the presence or absence of HAL1/13 antibody. The percentage of invading cells was then quantitated as described in *Methods*. Each bar represents mean $\pm$ SEM of 4-6 experiments. * denotes significant effect of hypoxia; ** denotes significant effect of HAL1/13-Ku antibodies

Figure 3. Confocal microscopy of endothelial cells invaded by neuroblastoma cells. Calcein-labeled neuroblastoma cells were co-incubated for 4 hours with a confluent monolayer of endothelial cells in 35 mm tissue culture dishes. The photographs of Kelly cells under normoxic (A), or hypoxic (B), conditions were taken at 17 microns from the apical surface of the endothelial cells.

Figure 4. Effect of hypoxia on transmigration of tumor cells through Matrigel-coated filters.

Kelly cells were subjected to hypoxia for 24 hours and MCF-7 cells for 48 hours. Cells were trypsinized and co-incubated with Matrigel-coated filters for 24 hours as described in *Methods*. Cells which transmigrated to the bottom chamber were labeled with calcein and their fluorescence was measured and related to the fluorescence of the total number of plated cells. Each bar represents mean $\pm$ SD of 3 experiments for each tumor cell line.

Figure 5. Effect of hypoxia on tumor cell motility. Videomicroscopy studies.

Kelly and MCF-7 cells were subjected to 24 and 48 hours of hypoxia respectively, trypsinized and plated onto laminin-coated surfaces as described in *Methods*. The image of the microscopic field was captured every minute. Coordinates of the cells in each image (usually 15-18 cells) were measured by means of NIH Image software, and the distance which each cell migrated during the time of observation (16 min) was calculated. A representative experiment with MCF-7 cells is shown in graph A. 16 cells per field were analyzed. Each diamond represents the distance migrated by one cell, and the bars are the mean distances. Graph B summarizes the mean distances migrated by normoxic or hypoxic tumor cells in the absence and presence of the antibody directed against HAL1/13. Each bar represents mean $\pm$ SEM of 4 experiments with Kelly cells and of 3 experiments with MCF-7 cells.

A

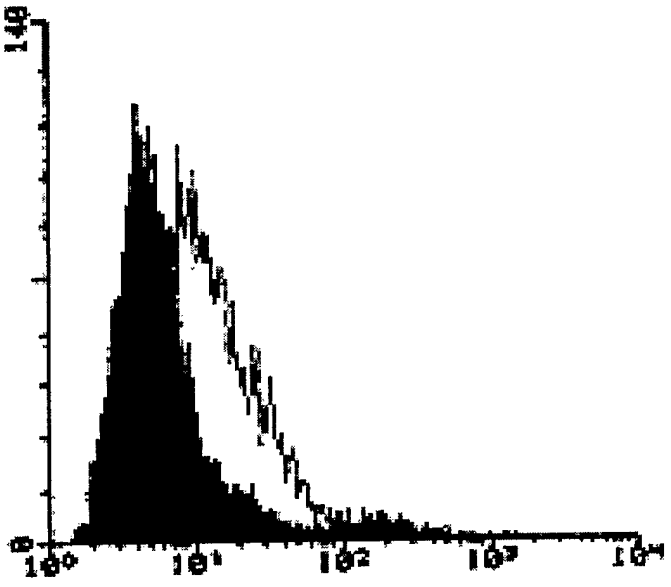

B

KELLY

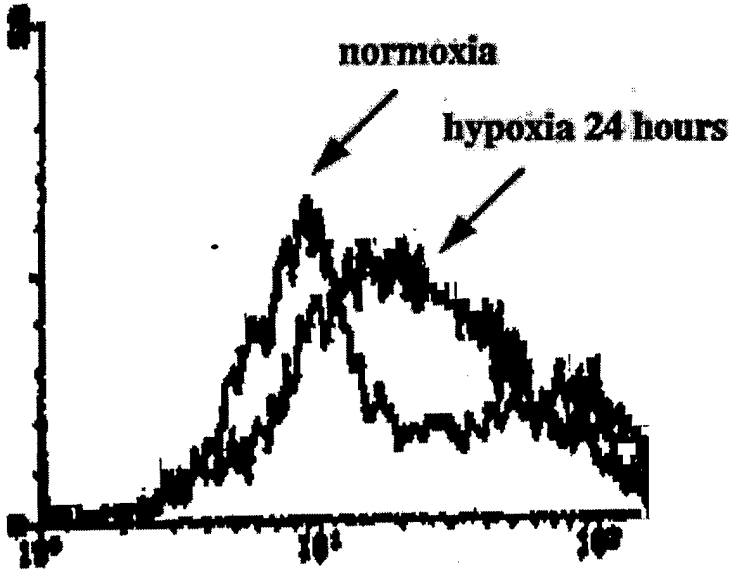

C

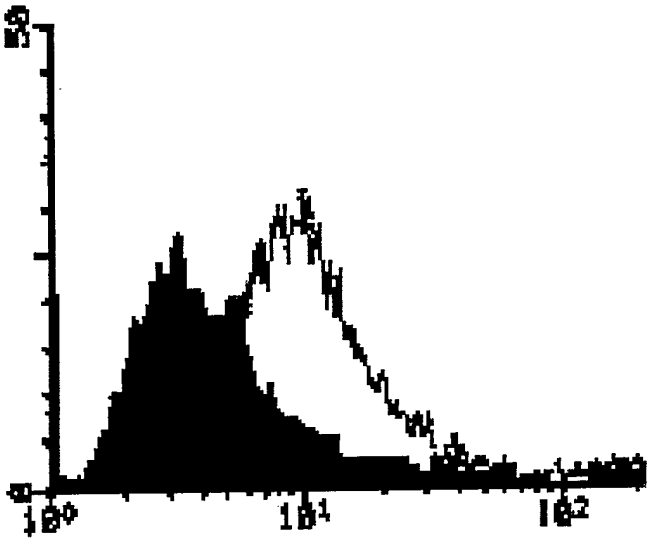

D

MCF-7

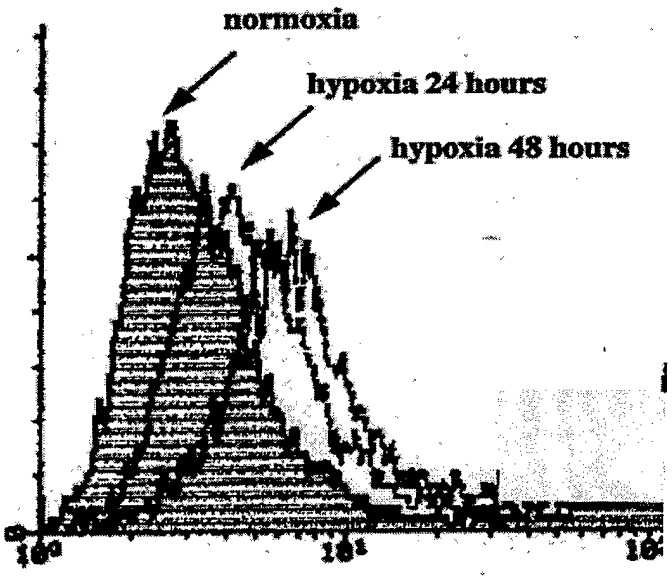

Ginis and Faller, Figure 1

Ginis and Faller. Figure 2

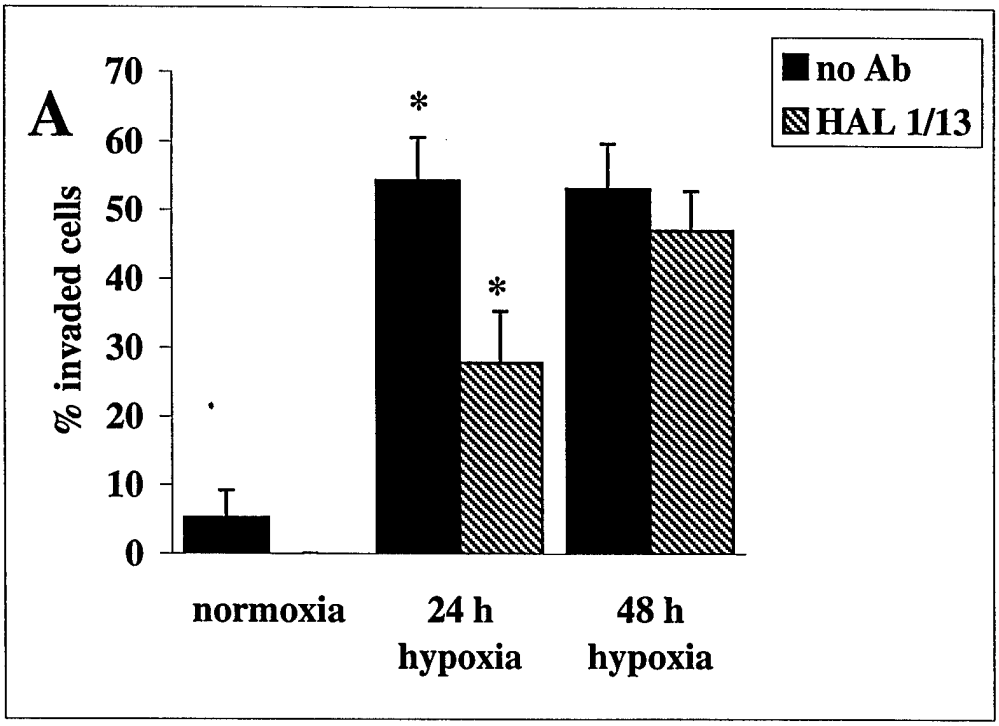

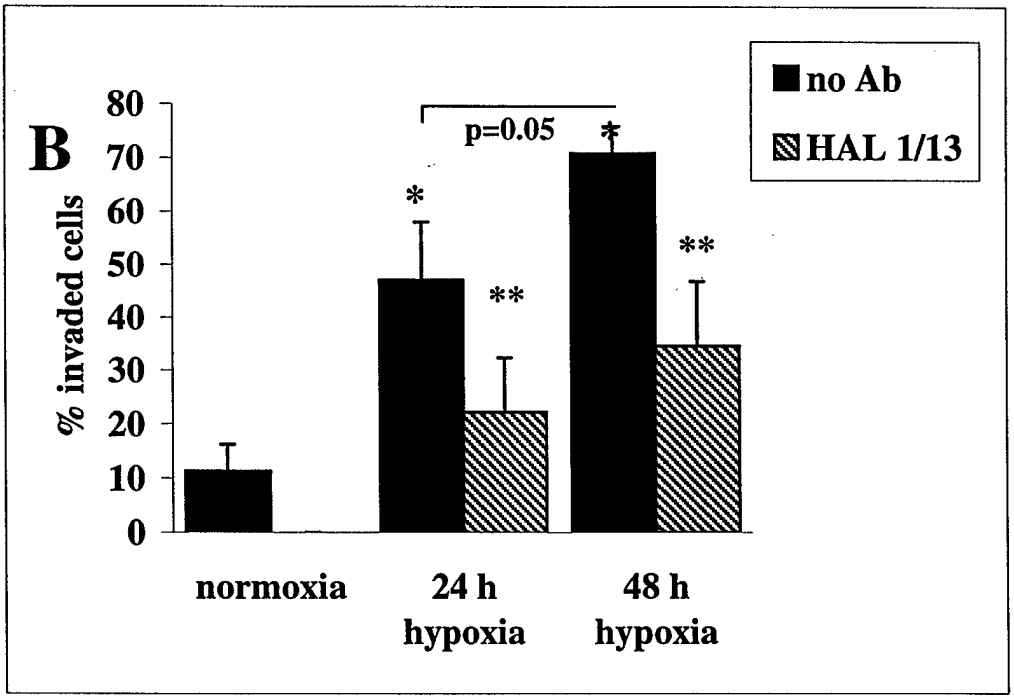

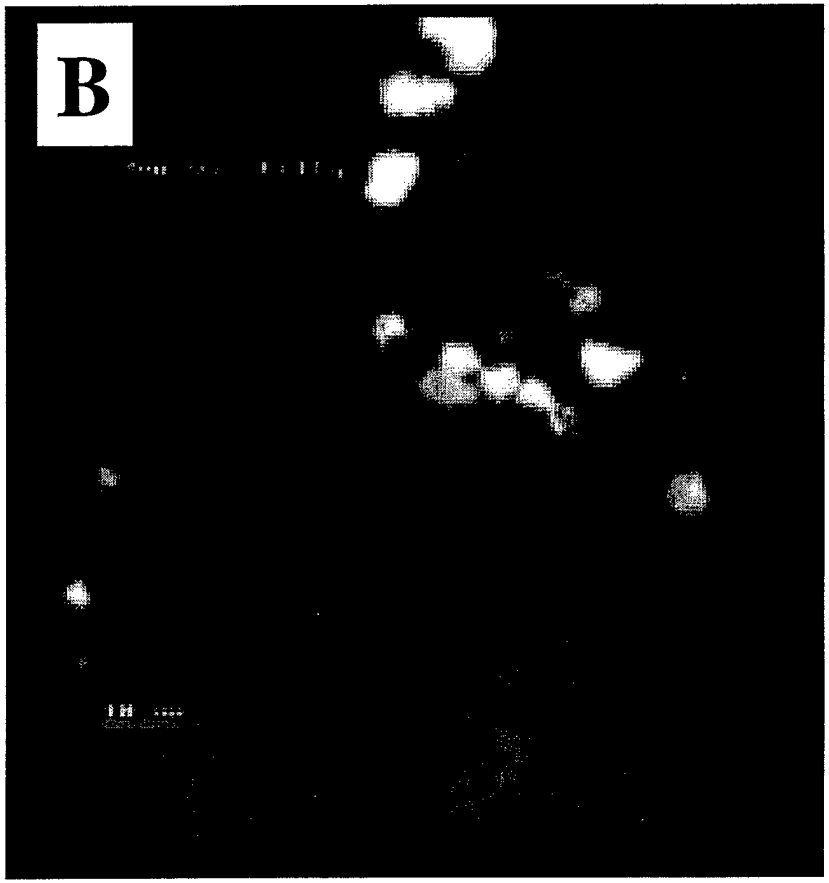

Ginis and Faller, Figure 3

Ginis and Faller. Figure 4

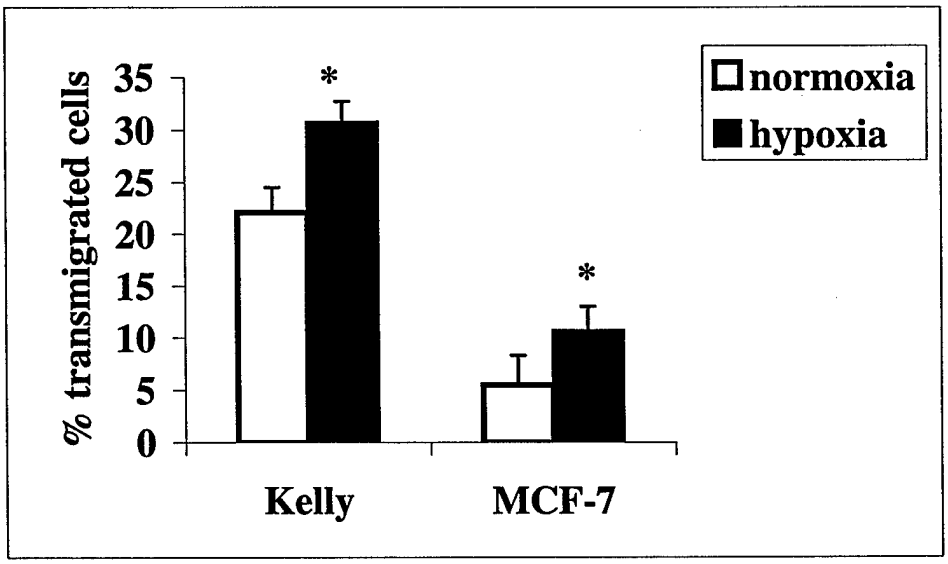

Ginis and Faller Figure 5

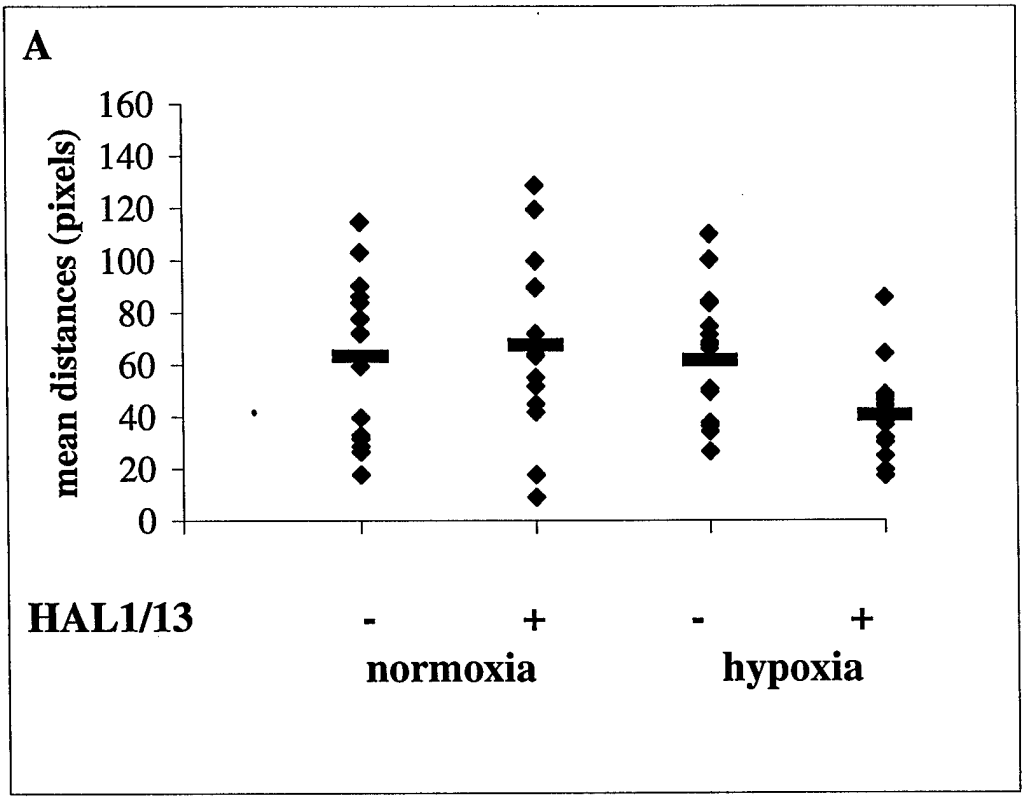

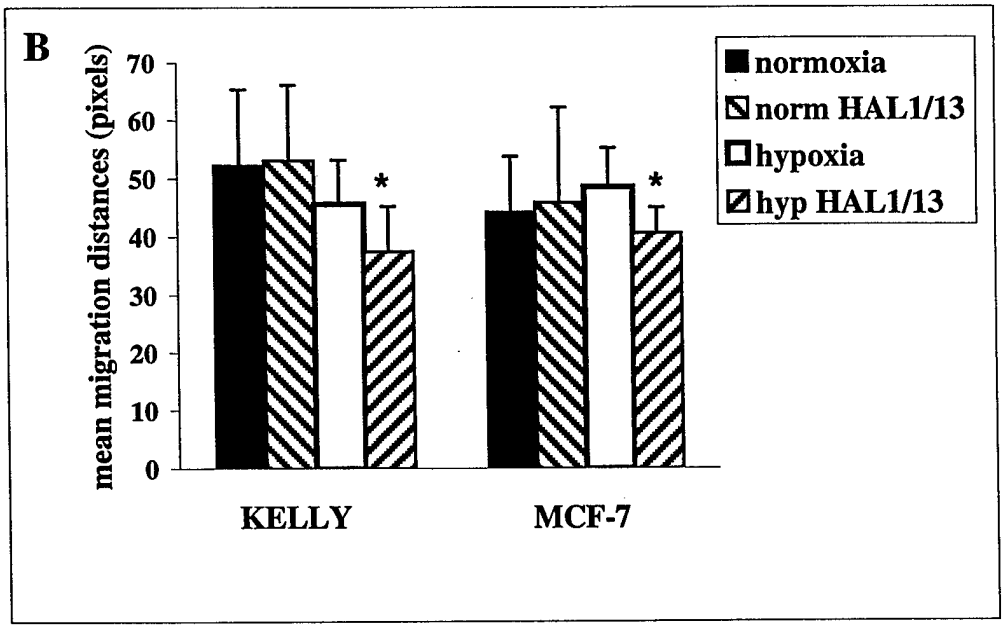

622
Faller, D.

The American Society of Hematology
Official Electronic Abstract Submission

Presenting Author: D. V. Faller
Address: Cancer Center, K-701, Boston Univ. School of MEdicine, 715 Albany St., Boston MA 02118, UNITED STATES (USA)
Phone: 617-638-4173 **Fax:** 617-638-4176 **E-mail:** dfaller@bu.edu
Sponsoring Author: D. V. Faller
Address: , ,
Phone: Fax: E-mail:
Filename: 434790
Abstract Category: 622
Presentation Preference? No preference
Special considerations:
Travel/Merit Award:
Disclosure Statement:
Payment Type: Electronic (complete)

TREATMENT OF EPSTEIN-BARR VIRUS (EBV)-ASSOCIATED LYMPHOMAS AND PTLD USING ARGININE BUTYRATE TO INDUCE VIRAL *TK* GENE EXPRESSION: INITIAL FINDINGS OF A PHASE I/II TRIAL.

D. V. Faller, Ph.D./M.D.[1], O. Hermine, M.D.*[2], T. Small, M.D.[3], R. O/Reilly, M.D.[3], J. Fingeroth, M.D.*[4], S. J. Mentzer, M.D.*[4], S. P. Perrine, M.D.[1]. [1]Cancer Research Center, Boston Univ. School of Medicine, Boston, MA, USA. [2]Hospital Necker, Paris, France. [3]Sloan-Kettering Cancer Center, NY, NY, USA. [4]Brigham and Women's Hospital, Boston, MA, USA.

Lymphoproliferative disorders associated with the Epstein-Barr virus (EBV) include non-Hodgkin's lymphoma and "post-transplant lymphoproliferative disorders" (PTLD), which occurs with immunosuppression after marrow and organ transplantation. PTLD is characterized by actively-proliferating EBV(+) B-lymphocytes and often manifests a rapidly progressive fatal clinical course if the immunosuppression cannot be reversed. A common treatment for Herpesvirus infections has targeted the virus-specific enzyme, thymidine kinase (TK). The lack of viral TK expression in EBV(+) tumor cells, due to viral latency, makes anti-viral therapy alone ineffective as an anti-neoplastic therapy, however. We have developed a strategy for treatment of EBV-associated lymphomas/PTLD using pharmacologic induction of the latent viral *TK* gene and enzyme in the tumor cells, followed by treatment with ganciclovir. Arginine Butyrate selectively activates the EBV *TK* gene in latently EBV-infected human lymphoid cells and tumor cells. A Phase I/II trial was therefore begun, employing an intra-patient dose escalation of Arginine Butyrate combined with ganciclovir. In six patients with EBV-associated lymphomas or PTLD, all of which were resistant to conventional radiation and/or chemotherapy, this combination produced complete clinical responses in 4/6 patients, with a partial response occurring in a fifth patient. Pathologic examination in 2/3 patients demonstrated complete necrosis of the EBV-lymphoma, with no residual disease, following a single three-week course of the combination therapy. Possible side-effects of the therapy included nausea and reversible lethargy at the highest doses. One patient suffered acute liver failure, thought to be secondary to release of FasL from the necrotic tumor. Analysis of patient-derived tumor cells in culture demonstrated that Arginine Butyrate produced selective induction of the EBV *TK* gene, which then conferred sensitivity to ganciclovir, resulting in tumor apoptosis. Additional patient accrual is sought for further evaluation of this therapy.

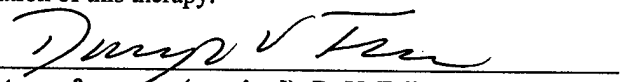

Signature of sponsor (required): D. V. Faller

203
Ginis, I.

The American Society of Hematology
Official Electronic Abstract Submission

Presenting Author: I. Ginis
Address: c/o Douglas Faller, Cancer Research Center, Boston Univ. School of Medicine, 715 Albany St., Room K-701, Boston MA 02118, UNITED STATES (USA)
Phone: 617-638-4173 **Fax:** 617-638-4176 **E-mail:** dfaller@bu.edu
Sponsoring Author: D. V. Faller
Address: Cancer Center, Boston University School of Medicine, 715 Albany St, K-701, Boston MA 02118, UNITED STATES (USA)
Phone: 617-638-4173 **Fax:** 617-638-4176 **E-mail:** dfaller@bu.edu
Filename: 438710
Abstract Category: 203
Presentation Preference? No preference
Special considerations:
Travel/Merit Award:
Disclosure Statement:
Payment Type: Electronic (complete)

THE HYPOXIA-ACTIVATED LIGAND HAL-1/13 IS IDENTICAL TO Ku80, AND MEDIATES LYMPHOID CELL ADHESION AND TUMOR CELL INVASIVENESS IN VITRO.

I. Ginis, Ph.D.*, E. Lynch, Ph.D.*, D. V. Faller, Ph.D./M.D., Cancer Research Center, Boston University School of Medicine, Boston, MA, USA.

Hematogenic spread of lymphoid tumor cells involves reversible interactions between adhesion receptors on lymphoid cells and their counterparts on vascular endothelium, surrounding tissues, and matrices, and closely resembles extravasation of lymphocytes and leukocytes to the sites of inflammation. Hypoxia is known to induce extravasation of lymphocytes and leukocytes during ischemic injury. Tumor hypoxia analogously increases the metastatic potential of malignant lymphoid cells. We have recently identified and characterized a new adhesion molecule, HAL-1/13 (Hypoxia-Activated Ligand-1/13), which mediates the increases in lymphocyte and neutrophil adhesion to endothelium under hypoxic conditions. We used expression-cloning to identify this molecule as the lupus antigen, and DNA-PK-associated nuclear protein, Ku80. The HAL-1/13/Ku80 antigen is found on the surface of many leukemic and solid tumor cell lines, including T and B lymphomas, myeloid leukemias, neuroblastoma, rhabdomyosarcoma, and breast carcinoma cells. Transfection and ectopic expression of (human) HAL-1/13/Ku80 on (murine) NIH-3T3 fibroblasts confers the ability of these normally non-adhesive cells to bind to a variety of human lymphoid cell lines, and this adhesion can be specifically blocked by HAL-1/13-neutralizing antibodies. Hypoxic exposure of lymphoma lines (Jurkat, JY), leukemia lines (U937), neuroblastoma (Kelly and SH-N-SK) and breast carcinoma (MCF-7) cells resulted in upregulation of HAL-1/13/Ku80 expression at the cell surface, mediated by translocation of the antigen from the nucleus. This upregulation was coincident with an increased ability of the tumor cells to invade endothelial monolayers, and this invasion could be attenuated by anti-HAL-1/13 antibody. Hypoxia also potentiated lymphoid tumor cell transmigration through Matrigel filters. Anti-HAL-1/13 antibody inhibited this transmigration, and also the locomotion of hypoxic tumor cells on laminin. These studies indicate that the HAL-1/13/Ku80 molecule may mediate, in part, the increased invasiveness of tumor cells induced by hypoxia, as well as regulating hypoxia-induced adhesion of normal lymphocytes and leukocytes to endothelial cells.

Dmyr V. Faller

Signature of sponsor (required): D. V. Faller

Final Report: Bibliography

Original Reports:

Mentzer, S.J., Fingeroth, J., Reilly, J.J., Perrine, S.P., and Faller, D.V. Arginine Butyrate-induced susceptibility to ganciclovir in an Epstein-Barr Virus (EBV)-associated lymphoma. *Blood Cells Molecules.Dis.* 24:114-123, 1998

Vaziri, C., Stice, L.L., and Faller, D.V. Butyrate-induced G1 arrest results from p21-independent disruption of retinoblastoma-mediated signals. *Cell Growth Differ.* 9:465-474, 1998.

Ginis I and Faller, DV. Hypoxia Affects Tumor Cell Invasiveness *In Vitro*: The Role of Hypoxia-Activated Ligand HAL1/13 (Ku 86 autoantigen)., 1999, *submitted for publication.*

Abstracts:

1. THE HYPOXIA-ACTIVATED LIGAND HAL-1/13 IS IDENTICAL TO Ku80, AND MEDIATES LYMPHOID CELL ADHESION AND TUMOR CELL INVASIVENESS IN VITRO. I. Ginis,* E. Lynch,* and D.V. Faller. Cancer Research Center, Boston University School of Medicine, Boston, MA American Society of Hematology Annual Meeting, 1999.

2. TREATMENT OF EPSTEIN-BARR VIRUS (EBV)-ASSOCIATED LYMPHOMAS AND PTLD USING ARGININE BUTYRATE TO INDUCE VIRAL *TK* GENE EXPRESSION: INITIAL FINDINGS OF A PHASE I/II TRIAL. D.V. Faller, O. Hermine,* T. Small, R. O'Reilly, J. Fingeroth,* S.J. Mentzer,* and S.P. Perrine. Cancer Research Center, Boston University School of Medicine, and Brigham and Women's Hospital, Boston, MA; Hospital Necker, Paris, France; Memorial-Sloan Kettering, New York, N.Y. American Society of Hematology Annual Meeting, 1999.

List of Personnel Receiving Support from the Research Effort:

Douglas V. Faller
Ai Leen Lam (2 months)
Lora W. Forman
Karyn Vandemark